



Article

---

# Physiological and Agronomic Responses of Adult Citrus Trees to Oxyfertigation Under Semi-Arid Drip-Irrigated Conditions

---

Juan M. Robles, Francisco Miguel Hernández-Ballester, Josefa M. Navarro, Elisa I. Morote, Pablo Botía and Juan G. Pérez-Pérez



## Article

# Physiological and Agronomic Responses of Adult Citrus Trees to Oxyfertigation Under Semi-Arid Drip-Irrigated Conditions

Juan M. Robles <sup>1,\*</sup>, Francisco Miguel Hernández-Ballester <sup>1</sup>, Josefa M. Navarro <sup>1</sup>, Elisa I. Morote <sup>1</sup>, Pablo Botía <sup>1</sup> and Juan G. Pérez-Pérez <sup>1,2</sup>

<sup>1</sup> Equipo de Riego y Fisiología del Estrés, Instituto Murciano de Investigación y Desarrollo Agrario y Medioambiental (IMIDA), 30150 La Alberca, Murcia, Spain; franciscom.hernandez4@car.m.es (F.M.H.-B.); josefam.navarro2@car.m.es (J.M.N.); elisai.morote@car.m.es (E.I.M.); pablo.botia@car.m.es (P.B.); perez\_juaperb@gva.es (J.G.P.-P.)

<sup>2</sup> Centro para el Desarrollo de la Agricultura Sostenible, Instituto Valenciano de Investigaciones Agrarias (IVIA), 46113 Moncada, Valencia, Spain

\* Correspondence: juanm.robles@car.m.es; Tel.: +34-968-366770

## Abstract

Oxyfertigation with hydrogen peroxide ( $H_2O_2$ ) has been successfully applied in several crops and production systems, but its use in mature citrus orchards under no-tillage conditions and semi-arid Mediterranean environments remains scarcely studied. This study aimed to evaluate the physiological responses of adult citrus trees and the agronomic performance of a mature citrus orchard subjected to chemical oxyfertigation based on the application of  $H_2O_2$  in irrigation water as an oxygen source for the root zone. The experiment was conducted over four consecutive seasons (2018–2021) on adult ‘Ortanique’ hybrid mandarin trees grown in an orchard located in Torre Pacheco (Murcia, Spain). Two treatments were established: a ‘Control’ (0 mg  $L^{-1}$  of  $H_2O_2$ ) and an ‘OXY’ treatment (50–100 mg  $L^{-1}$  of  $H_2O_2$  applied throughout the growing season). Oxyfertigation significantly increased the dissolved oxygen in irrigation water and soil oxygen diffusion rate, with treatment and treatment  $\times$  time effects showing greater oxygenation under conditions favoring transient root-zone hypoxia. Soil  $CO_2$  and  $H_2O$  vapor fluxes exhibited marked seasonal dynamics but no consistent treatment effect, and soil salinity and macro- and micronutrient contents were not significantly altered. At the plant level, oxyfertigation episodically enhanced leaf gas exchange and transiently improved the water status, but did not produce a sustained increase in leaf-level water use efficiency. In contrast, OXY trees showed greater pruning biomass, more fruits (+18%), higher cumulative yield (+13%), and significantly higher crop water use efficiency (YWUE) while the mean fruit weight and most quality attributes were governed by interannual climatic variability. In summary, oxyfertigation acted as a complementary and safe agronomic practice that improved rhizosphere oxygenation and supported modest gains in fruit load and YWUE in mature citrus orchards.



Academic Editor: Chengfang Li

Received: 19 November 2025

Revised: 15 December 2025

Accepted: 25 December 2025

Published: 29 December 2025

**Copyright:** © 2025 by the authors.

Licensee MDPI, Basel, Switzerland.

This article is an open access article distributed under the terms and conditions of the [Creative Commons Attribution \(CC BY\) license](#).

**Keywords:** hydrogen peroxide; dissolved oxygen; ODR; water relations; pruning biomass; yield; fruit number; crop water-use efficiency; fruit quality

## 1. Introduction

Spain is one of the leading citrus-producing countries in the Mediterranean basin, with production mainly concentrated in the regions of Valencia, Andalusia, and Murcia (MAPA 2025) [1]. In the Region of Murcia, citrus cultivation (after vegetables) represents

one of the most important crops from a socioeconomic standpoint. During the 2023 season, production reached 706,445 t of lemon, 112,429 t of orange, and 98,253 t of mandarin fruits [2]. The climate in this area is semi-arid, and under these conditions, the viability of agricultural farms mainly depends on the efficient management and availability of existing water resources. For this reason, irrigation and crop management aimed at maximizing crop water use efficiency (YWUE) [3], defined as the fruit yield per unit of irrigation water applied ( $\text{kg m}^{-3}$ ), are of great importance in this region.

One practice that has been proposed to improve crop yield and YWUE is an irrigation strategy known as aerated irrigation [4,5]. Oxygen availability may become a primary limiting growth factor under specific soil conditions such as waterlogging, compaction, or poor aeration [6], whereas under well-aerated soils, its role is secondary, in agreement with Liebig's law of the minimum. For proper crop development, the presence of  $\text{O}_2$  in the soil solution is essential since roots require adequate  $\text{O}_2$  concentrations to function properly and to meet the water and nutrient demands of the aerial parts of the plant [7,8]. However, certain situations can cause  $\text{O}_2$  deficiency in the soil, leading to reduced crop productivity [9]. The main causes include the use of low-quality water with high salinity [10], soil compaction due to the absence of tillage [11], and waterlogging caused by excessive irrigation or torrential rains in heavy clay soils [12].

Soil–root aeration in irrigated systems is governed predominantly by diffusion:  $\text{O}_2$  moves first through air-filled pores and, after infiltration events, across thin water films where its diffusivity is ~10,000 times lower than in air. Consequently, soil texture, structure, and irrigation frequency strongly condition rhizosphere  $\text{O}_2$  supply [13,14]. Classical field work introduced the  $\text{O}_2$  diffusion rate (ODR) as a practical proxy for root-zone aeration and reported method-dependent thresholds for growth cessation under low  $\text{O}_2$  supply. Later mechanistic models showed that no universal critical ODR value exists since aeration requirements depend on temperature, root length density, microbial respiration, and the depth and distribution of active sinks [15–18]. At the plant level, root hypoxia triggers coordinated metabolic and anatomical acclimations responses, including a shift towards fermentative metabolism, ethylene signaling, and the formation of aerenchyma and barriers to radial  $\text{O}_2$  loss, which enhance internal gas transport and tolerance to episodic  $\text{O}_2$  limitation in irrigated soils [19–21]. In drip-irrigated crops, transient saturation in the wetted bulb around emitters can depress soil  $\text{O}_2$  immediately after irrigation. This has motivated the development of oxygen-enrichment strategies to characterize and alleviate short-term aeration constraints in the root zone [14,22,23].

Under conditions where gas exchange in the soil may be restricted, maintaining adequate  $\text{O}_2$  levels in the root zone may represent an additional agronomic constraint that interacts with other stresses rather than a uniquely limiting factor. To mitigate this constraint, the application of  $\text{O}_2$ -releasing products has emerged as an effective complementary strategy. These products help maintain high concentrations of  $\text{O}_2$  in the rhizosphere throughout the crop cycle, supporting root functioning under suboptimal aeration. As a result, they can promote plant growth and yield while improving both water and fertilizer use efficiency [4,24].

Hydrogen peroxide ( $\text{H}_2\text{O}_2$ ) is applied in oxyfertigation to enrich dissolved  $\text{O}_2$  in the root zone [25]. Its decomposition yields water and oxygen via catalase and metal-mediated disproportionation ( $2\text{H}_2\text{O}_2 \rightarrow 2\text{H}_2\text{O} + \text{O}_2$ ), and can also generate hydroxyl radicals through Fenton-type reactions ( $\text{Fe}^{2+} + \text{H}_2\text{O}_2 \rightarrow \text{Fe}^{3+} + \bullet\text{OH} + \text{OH}^-$ ) that contribute to rhizosphere sanitization and organic matter oxidation. In drip-irrigated orchards, these processes can transiently improve rhizosphere aeration and root activity [25]. Additionally,  $\text{H}_2\text{O}_2$  can also be used in drip irrigation systems to control biofouling and remove scale formation in emitters, as demonstrated by Tachikawa and Yamanaka [26], and in systems using treated

wastewater [27]. The effects of applying  $\text{H}_2\text{O}_2$  via irrigation clearly depend on the crop species, substrate, and environmental context. In hydroponic and soilless systems, the results have been mixed: in strawberry plants,  $\text{H}_2\text{O}_2$  application has increased the yield and fruit number during the late production stage [28], while in soilless-grown pepper, oxyfertigation has improved yield under commercial greenhouse conditions [29,30]. By contrast, Acuña et al. (2006) [31] reported no significant effects of  $\text{H}_2\text{O}_2$  in perlite-grown plants, highlighting that substrate properties and baseline aeration critically modulate the response. In soil-based systems, particularly in fine-textured or poorly aerated soils, the evidence is more consistently positive. The application of  $\text{H}_2\text{O}_2$  has increased the total biomass and yield of zucchini [32] and pepper [25]. Similar improvements have been reported in potted crops such as soybean and cotton, showing higher biomass and productivity [32]. In potato, irrigation water oxygenation with  $\text{H}_2\text{O}_2$  has improved growth, physiological performance, and tuber yield under optimal irrigation and helped mitigate drought stress in poorly aerated clay-loamy soils [33]. More recently, moderate concentrations of  $\text{H}_2\text{O}_2$  ( $600\text{--}800\text{ mg L}^{-1}$ ) have been shown to improve soil aeration, antioxidant enzyme activity, and grain yield in winter wheat, with yield gains of up to 25% relative to non-oxygenated irrigation [34].

Research on the effects of  $\text{H}_2\text{O}_2$  in woody crops is still limited, and the available studies have reported variable responses depending on the species, soil type, and irrigation conditions. In avocado,  $\text{H}_2\text{O}_2$  application in poorly drained soils has increased plant biomass and crop water use efficiency (YWUE) without significantly affecting  $\text{CO}_2$  assimilation, transpiration, stomatal conductance, or stem water potential while the xylem vessel diameter and the xylem/phloem ratio has tended to be greater in treated trees [35]. In grapevine, Thomas et al. [25] conducted a four-year field study and found that the addition of 10 ppm  $\text{H}_2\text{O}_2$  consistently increased the yield by about 25%, particularly in the later years of the experiment. In citrus,  $\text{O}_2$  availability in the soil solution is critical for proper root development and nutrient uptake [36]. Ben-Noah et al. [37] evaluated soil air injection in mature 'Valencia' orange trees under shallow groundwater conditions and, although soil  $\text{O}_2$  levels slightly increased, they did not observe significant changes in tree growth, yield, or fruit quality.

Therefore, despite the promising evidence of  $\text{H}_2\text{O}_2$  application in other crops and production systems, its effects as an oxygen-enriching additive in mature citrus orchards under semi-arid Mediterranean conditions remain insufficiently documented. Based on this knowledge gap, the present study did not assume the existence of an a priori  $\text{O}_2$  deficiency in the root zone, but instead aimed to evaluate the functional response of the soil-plant system to increased dissolved  $\text{O}_2$  in irrigation water through  $\text{H}_2\text{O}_2$  application. We hypothesized that  $\text{O}_2$ -enriched irrigation could modify soil aeration dynamics and influence root activity and plant physiological performance and, ultimately improve productivity and YWUE under field conditions. The specific objectives of this study were to (1) assess the effects of oxyfertigation on soil chemical and biological characteristics; (2) evaluate its physiological impact on leaf  $\text{CO}_2$  assimilation, transpiration, stomatal conductance, and stem water potential; and (3) quantify its effects on yield, crop water use efficiency, and fruit quality in comparison with a control treatment.

## 2. Materials and Methods

### 2.1. Experimental Conditions and Plant Material

The experimental site was located at the IMIDA experimental station in Torre Pacheco (Murcia, Spain), under a semi-arid Mediterranean climate characterized by mild winters and hot, dry summers. Meteorological data were obtained daily by an automatic weather station installed within the orchard (station TP-91 of the Servicio de Información Agraria de

Murcia, SIAM-IMIDA). Over the four-year study (2018–2021), mean daily solar radiation was of  $18.5 \text{ MJ m}^{-2} \text{ day}^{-1}$  and mean annual air temperature was  $17.9^\circ\text{C}$ , with seasonal extremes ranging from  $4\text{--}8^\circ\text{C}$  in winter to  $32\text{--}38^\circ\text{C}$  in summer. Annual rainfall averaged 384 mm, but varied markedly among years (304 mm in 2018 to 512 mm in 2019), with most precipitation concentrated in autumn and winter. Reference evapotranspiration ( $ET_0$ , calculated using the Penman–Monteith method [38,39]) ranged from 1138 to 1246 mm per year, reflecting high atmospheric demand during summer months. Irrigation water supplied by the *Campo de Cartagena* community had an average electrical conductivity (EC) of  $1.28 \text{ dS m}^{-1}$ , typical of moderately saline water in the region. The soil was classified as sandy clay loam (23% clay, 26% silt, 51% sand), with a bulk density of  $1.4 \text{ g cm}^{-3}$ , pH 7.9, EC  $0.36\text{--}0.41 \text{ mS cm}^{-1}$ , organic matter content of 2.02%, and 11.02% active  $\text{CaCO}_3$ . The orchard consisted of 25-year-old ‘Ortanique’ mandarin trees under no-tillage conditions, drip-irrigated since establishment, and managed according to integrated production standards for citrus in Murcia.

All plant material used in this study consisted of *Citrus reticulata* Blanco  $\times$  *Citrus sinensis* (L.) Osbeck ‘Ortanique’ hybrid mandarin trees grafted onto ‘Carrizo’ citrange (*Citrus sinensis* Osb.  $\times$  *Poncirus trifoliata* (L.) Raf.) rootstock. The orchard (1 ha, with a tree-spacing of  $3 \times 4 \text{ m}$ ) was originally established in 1993 using certified nursery trees supplied by a commercial citrus nursery in the Region of Murcia (Spain). Trees were propagated exclusively by conventional grafting (T-budding) onto standard rootstock seedlings. No micropropagation or tissue-culture techniques were used at any stage of plant production. All trees within the experimental orchard were of the same origin, age, and propagation method, ensuring genetic and horticultural uniformity across treatments.

Each tree row was equipped with a single drip line containing three Netafim<sup>TM</sup> self-compensating drippers (Netafim<sup>TM</sup>; Netafim Ltd., Kibbutz Hatzerim, Israel) delivering  $4 \text{ L h}^{-1}$  per tree. Crop evapotranspiration ( $ET_c$ ) were calculated following the FAO-56 method [39], using  $ET_0$  data from the on-site station, and the crop coefficient ( $K_c$ ) values used were those provided by “Servicio de Información Agraria de Murcia (SIAM-IMIDA)” for late-season mandarin cultivars. Irrigation and fertigation were controlled automatically by a central head unit (Xilema NX300; Novedades Agrícolas S.A., Torre Pacheco, Spain), equipped with electro-hydraulic valves (uPVC; Regaber S.A., Parets del Vallès, Spain), applying the same fertilization program and irrigation dose (100%  $ET_c$ ) across treatments. Irrigation frequency varied seasonally, from twice in winter to daily in summer, for both treatments. The volume of water applied was monitored using flowmeters. Fertigation totals, formulations, and timing were identical for all trees and seasons (2018–2021) and were supplied from the same head unit.

All orchard management practices, including irrigation scheduling, fertigation, pest and disease control, and pruning, were those commonly used by growers for late-harvested mandarin cultivars in the area according to technical standards of integrated production in the citrus cultivation in the Region of Murcia [40]. These practices were applied identically to all trees, using the same active ingredients, doses, and application dates. All interventions were recorded by field staff, and detailed logs are available upon request. Pruning was carried out manually after the harvest in late winter to minimize the risk of frost damage.

Two treatments were established: a ‘Control’ treatment— $0 \text{ mg L}^{-1}$  of  $\text{H}_2\text{O}_2$  in drip irrigation water—and an ‘OXY’ treatment:  $50\text{--}100 \text{ mg L}^{-1}$  of  $\text{H}_2\text{O}_2$  in irrigation water, adjusted to maintain  $20\text{--}30 \text{ mg L}^{-1}$  dissolved  $\text{O}_2$  (DO) at the dripper outlet throughout the crop cycle). These ranges of  $\text{H}_2\text{O}_2$  and the target of dissolved  $\text{O}_2$  were selected based on published guidelines for drip applications reporting physiological benefits without phytotoxicity [25] and on our preliminary orchard trials, which confirmed emitter integrity and the absence of oxidative damage at these doses. The  $\geq 20 \text{ mg L}^{-1}$  DO target was

consistent with oxygenated irrigation studies documenting improved plant performance around this concentration [41] and with technical reports showing that supersaturation up to approximately 30 mg L<sup>-1</sup> is feasible in pressurized irrigation lines [42]. H<sub>2</sub>O<sub>2</sub> was injected continuously using a digital membrane dosing pump during each irrigation event in the OXY treatment to reach a target dose of 50–100 mg L<sup>-1</sup> at the head unit. The injection rate (L h<sup>-1</sup>) was calculated from system flow and target mg L<sup>-1</sup> using this conversion:

$$\text{Injection rate (L h}^{-1}\text{)} = \text{system flow (m}^3 \text{ h}^{-1}\text{)} \times \text{target (mg L}^{-1}\text{)}/(\% \text{ stock, } w/w) \times 10$$

The experimental design consisted of four completely randomized blocks, each with two treatments and three monitored trees per treatment (12 trees per treatment in total). Each block consisted of three adjacent rows with five trees per row (15 trees in total). The three trees located in the central row were used as experimental units while the remaining trees served as border trees to prevent edge interference. Additionally, blocks assigned to different treatments were separated by at least one complete tree row (4 m), acting as a buffer to minimize spatial autocorrelation and possible edaphic or microclimatic gradients between treatments. This configuration was chosen to maintain locally homogeneous conditions within blocks, ensure adequate spatial independence among treatment plots, and allow a robust evaluation of treatment effects at the individual tree level.

## 2.2. Measurements

### 2.2.1. Dissolved Oxygen (DO) and Soil Oxygen Diffusion Rate (ODR)

DO in irrigation water was monitored periodically during the main irrigation season (May–October) in 2020 and 2021. Measurements were taken *in situ* at the dripper outlet under steady-state flow conditions, approximately midway through irrigation events. DO was recorded in the four replicate plots per treatment using a portable DO meter (HI9147-04; Hanna Instruments, Woonsocket, RI, USA) following the manufacturer's specifications for calibration and temperature compensation. The meter specifications were thus: range 0.0–50.0 mg L<sup>-1</sup> and 0–600% O<sub>2</sub> saturation; resolution 0.1 mg L<sup>-1</sup> (1%); accuracy  $\pm 1\%$  of reading; automatic temperature compensation; manual one-point calibration in saturated air; salinity compensation (0–51 g L<sup>-1</sup>); and altitude compensation (up to 4000 m). A one-point calibration in saturated air was performed daily at the measurement site, and salinity and local altitude were set according to site conditions. To capture potential DO gradients along the distribution network, readings were taken both at the dripper outlet and at the distal end of the lateral line.

ODR was measured periodically between May and September in 2020 and 2021, in twelve trees per treatment. Measurements were taken near the drippers within the wetted zone at rooting depth and immediately after irrigation (9:00–11:00 a.m.), when transient O<sub>2</sub> limitation is most likely. Readings were made with a Pt microelectrode and an Ag/AgCl reference electrode using an ODR meter (model 14.36.03; Royal Eijkelkamp, Giesbeek, The Netherlands), following the manufacturer's operating procedure and reading the steady-state diffusion-limited current after stabilization [43]. The system applied a stabilized potential and recorded the current required to reduce O<sub>2</sub> at the Pt surface; measuring range: 0–999  $\mu$ A (resolution 1  $\mu$ A) with accuracy  $\pm 3\mu$ A; operating temperature: 0–50 °C. Prior to field measurements, the Ag-AgCl reference electrode was cleaned and generated, and instrument checks were performed as described by the manufacturer.

### 2.2.2. Soil Physicochemical and Microbiological Analyses

Soil physicochemical and microbiological analyses were conducted in October 2020 and 2021. Four soil samples per treatment (one per block between three trees) were collected from the rhizosphere (10–30 cm depth, 10–15 cm from the dripper) using a mechanical

auger. Samples were kept at low temperature and analyzed following ISO and UNE standards. Electrical conductivity was measured in an aqueous extract (1:5) at 25 °C using a conductivity meter (Seven2Go S7; Mettler-Toledo, Columbus, OH, USA). The exchange cations (Na, K, Ca, and Mg) were extracted using BaCl<sub>2</sub> (standard method ISO 11260:2018) and measured by inductively coupled plasma atomic emission spectroscopy (ICP-OES; Vista MPX; Varian Inc., Palo Alto, CA, USA) (standard method ISO 22036:2008). The pH was determined in a 1:2 extract with 1 M KCl (ISO 10390:2021), using a pH-meter, (Seven2Go S8; Mettler-Toledo, Columbus, OH, USA). Active limestone was measured after the extraction with ammonium oxalate, using a Bernard calcimeter (PRIMACS SNC-100; Skalar Analytical B.V., Breda, The Netherlands) (method UNE 103200:2021). Organic matter and oxidizable organic carbon were determined by oxidation with dichromate using the Walkley–Black method [44]. The aqueous extraction of soluble anions (NO<sub>3</sub><sup>−</sup>, NO<sub>2</sub><sup>−</sup>, SO<sub>4</sub><sup>2−</sup>, PO<sub>4</sub><sup>3−</sup>) was performed as indicated in the standard method UNE-EN 13652:2002, and the concentrations were determined by liquid-phase ion chromatography (Eco IC; Metrohm AG, Herisau, Switzerland) (standard method UNE-EN ISO 10304-1:2009). The extraction and determination of exchange cations was conducted as described previously via extraction using BaCl<sub>2</sub> and determination by ICP-OES. The cation exchange capacity (CEC) was calculated using the method of summation of bases plus the exchangeable acidity (Al<sup>3+</sup> + H<sup>+</sup>) [45]; N was analyzed according to the Kjeldahl method by potentiometric titration (PTA-FQ-020).

In the soil samples, the abundance of several functional groups of soil microorganisms was determined by counting the number of aerobic mesophiles, molds and yeasts, and actinomycetes with the plate count method. To quantify the aerobic mesophiles, soil samples were sown in PCA (plate count agar) culture medium and incubated at 30 °C for 72 h, and visible colonies were counted (UNE-EN ISO 4833). In order to quantify the molds and yeasts, soil samples were sown in DRBC culture medium and incubated at 25 °C for 2–3 days, and the colonies that could be differentiated were counted (ISO-21527). To quantify the actinomycetes, soil samples were sown in AIA (actinomycetes isolation agar) culture medium and incubated at 30 °C for 7 days. Visible colonies were counted (Standard Method 9250 [Detection of Actinomycetes]). Phytopathology nematodes were analyzed in the same samples. Nematodes were extracted from soil samples by elutriation using an Oostenbrink disc after sieving through a series of meshes [46]. Extracted nematodes were concentrated by centrifugation and counted under a stereomicroscope; representative specimens were mounted in glycerine and identified to genus or species level under a compound microscope.

### 2.2.3. Soil Respiration

Soil respiration (CO<sub>2</sub> and H<sub>2</sub>O vapor fluxes) was measured between June and October in 2020 and 2021. Measurements were periodically conducted between 11:00 a.m. and 12:00 p.m. using a portable soil respiration system (LI-8100A Infrared Gas Analyzer; LI-COR Biosciences, Lincoln, NE, USA) equipped with a 20 cm diameter survey chamber. For this purpose, 24 polyvinyl chloride (PVC) collars (20 cm in diameter and 10 cm in height) were installed in the moist zone influenced by the irrigation bulb. Twelve collars corresponded to the Control treatment and the remaining twelve to the OXY treatment. Measurements with the LI-8100A quantified total soil CO<sub>2</sub> efflux (sum of autotrophic root and heterotrophic microbial respiration). No respiratory partitioning (e.g., root exclusion or isotopic methods) was performed; fluxes are therefore interpreted as rhizosphere activity rather than root-specific respiration.

#### 2.2.4. Midday Stem Water Potential

Midday stem water potential ( $\Psi_{\text{stem}}$ ) was measured every two weeks during the main irrigation season over the experimental period (2018 to 2021), on one mature, fully-expanded leaf from the middle third of each tree, in twelve trees per treatment. Leaves were enclosed within foil-covered plastic and aluminum envelopes at least 2 h before the midday measurement [47]. The  $\Psi_{\text{stem}}$  value was measured at noon with a pressure chamber (model 3000; Soil Moisture Equipment. Corp., Santa Barbara, CA, USA), following the recommendations of Turner [48].

#### 2.2.5. Leaf Gas Exchange

Leaf gas exchange measurements were taken on the same dates as  $\Psi_{\text{stem}}$ , between 08:00 and 10:00 GMT, under daylight hours (to avoid high afternoon temperatures and air vapor pressure deficit). Measurements were taken on healthy, sun-exposed mature leaves (one leaf per tree, twelve trees per treatment). Net photosynthesis rate ( $A_{\text{CO}_2}$ ), stomatal conductance ( $g_s$ ), and leaf transpiration rate ( $E_{\text{leaf}}$ ) were determined using a portable photosynthesis system (Li-6400, Li-Cor, Lincoln, NE, USA) equipped with a broad leaf chamber ( $6.0 \text{ cm}^2$ ). Instantaneous ( $A_{\text{CO}_2}/E_{\text{leaf}}$ ) and intrinsic ( $A_{\text{CO}_2}/g_s$ ) leaf water use efficiency and intercellular  $\text{CO}_2$  concentration ( $C_i$ ) were calculated automatically by the internal software program of the Li-6400, based on the equations of Von Caemmerer and Farquhar [49]. The air flow rate inside the leaf chamber was  $500 \mu\text{mol s}^{-1}$ . At the beginning of the measurements, each day, the temperature of the block of the leaf chamber was fixed using the air temperature reference ( $15\text{--}26^\circ\text{C}$ ). Portable 12 g cartridges of high-pressure, liquefied, pure  $\text{CO}_2$  were attached to the console by an external  $\text{CO}_2$  source assembly and were controlled automatically by a  $\text{CO}_2$  injector system (6400-01 LiCOR, Lincoln, NE, USA). The reference  $\text{CO}_2$  concentration was fixed at  $400 \mu\text{mol mol}^{-1}$ . All of the measurements were made using a red–blue light source (6400-02B light emitting diode; Li-COR, Lincoln, NE, USA) attached to the leaf chamber, and the PPF was fixed at the average value of the natural daylight at the time of measurement,  $1200 \mu\text{mol m}^{-2} \text{ s}^{-1}$ , which exceeded the saturating light intensity for photosynthesis of citrus leaves [50,51] but was not enough to provoke photoinhibition [52].

#### 2.2.6. Leaf Mineral Composition

Leaf mineral composition was analyzed annually in November throughout the experimental period (2018 to 2021). The leaf samples consisted of 25 fully mature leaves (5–8 months old) from each tree from twelve trees per treatment ( $n = 12$  trees per treatment per year). For each tree, the 25 leaves were pooled into a single composite sample and processed jointly. Leaves were washed, oven-dried ( $60^\circ\text{C}$ ), ground, and sieved (5 mm). Macronutrients (N, P, K, Ca, Mg, Na, and Cl) and micronutrients (Fe, Cu, Mn, and Zn) were determined. The dried and ground leaf tissue was ashed at  $550^\circ\text{C}$  and dissolved in  $\text{HNO}_3$  to determine the presence of P, K, Mg, Ca, Na, Fe, Cu, Mn, and Zn by inductively coupled plasma atomic emission spectroscopy (Varian MPX Vista; Palo Alto, CA, USA). Total N was determined by a direct combustion nitrogen analyzer (Model FP-428; Leco Corporation, St. Joseph, MI, USA).

#### 2.2.7. Vegetative Growth

Vegetative growth was monitored by measuring trunk diameter at a fixed height (30 cm above the graft union) using permanent band dendrometers (Model D1, UMS GmbH, München, Germany) installed on twelve trees per treatment. The trunk cross-sectional area (TCSA,  $\text{cm}^2$ ) was calculated as  $\pi \times (\text{diameter}/2)^2$ , and the absolute growth rate of the TCSA ( $\text{AGR}_{\text{trunk}}$ ) was derived from seasonal increments [53]. At the end of each

crop season, and in the same trees, the individual fresh pruning weight ( $\text{kg tree}^{-1}$ ) was measured with a portable digital scale.

#### 2.2.8. Root Biomass

Root biomass was evaluated at the end of the experiment (November 2021). Samples were collected within the wetted bulb zone, near the drip emitter, from four trees per treatment (one per block). Soil cores were extracted using a Royal Eijkelkamp E53 soil sampling ring kit (Royal Eijkelkamp, Giesbeek, The Netherlands) equipped with an auger and a closed ring holder to obtain undisturbed samples. Stainless-steel rings (53 mm diameter  $\times$  51 mm height; 100  $\text{cm}^3$  volume) with a sharpened lower edge were used to facilitate insertion and minimize friction and disturbance. Sampling was conducted at two depths (15 and 35 cm) after removing surface plant residues to avoid contamination. Samples were labeled, stored at 4 °C, and processed within 24–48 h to prevent degradation of fine roots. Each soil core was gently disaggregated onto a set of standardized sieves (ISO 3310-1:2016; 300 mm diameter) arranged in decreasing mesh size (2 mm, 1 mm, and 0.1 mm). Water washing facilitated separation, cleaning, and recovery of fine and coarse root fractions. Roots retained on each sieve were separated using tweezers and a soft brush and subsequently placed in water-filled trays for diameter classification. Roots  $\geq$  2 mm in diameter (retained on the 2 mm sieve) were classified as thick roots whereas those  $<2$  mm (retained on the 1 mm sieve) were classified as fine roots. Each root fraction was placed in a labeled container, and non-root or foreign material was manually removed. Samples were drained, blotted with filter paper, and air-dried to remove surface moisture. Fresh weight was then recorded. For dry weight determination, fine and thick root fractions were placed in paper envelopes and oven-dried at 60 °C for 48–72 h. Dried samples were cooled in a desiccator and weighed using a precision balance (GRAM FV-220, Gram Precision, Barcelona, Spain).

#### 2.2.9. Yield and Fruit Quality

Fruit yield was determined throughout the experimental period by harvesting and counting all fruits from each monitored tree at commercial maturity (February–March), following EU Regulation No. 1799/2001 [54]. Measurements were performed on twelve trees per treatment. The total fruit weight per tree was recorded using a digital scale, and mean fruit weight was calculated by dividing the total fruit weight by the number of fruits per tree. Crop water use efficiency (YWUE) was calculated as the ratio of yield to total irrigation water applied.

At harvest, a sample of nine commercial fruits were collected from each of the twelve trees per treatment (108 fruits per treatment) to analyze fruit quality. In each fruit, the external peel color was measured using a tri-stimulus color difference meter (Minolta CR-300, Konica-Minolta Sensing, Osaka, Japan) at three locations around the equatorial plane of the fruit. The Hunterlab parameters  $L$ ,  $a^*$ , and  $b^*$  were used, and the external color index (ECI) was calculated using the following equation:

$$\text{ECI} = (a^* \times 1000) / (L \times b^*), \quad (1)$$

where  $L$  indicates lightness and  $a^*$  and  $b^*$  are the chromaticity coordinates. ECI has a high correlation with the visual appreciation of the fruit color and ranges from negative (green) to positive (orange–red). Fruits were cut in the equatorial plane, and peel thickness was measured at three points with a digital caliper. For each tree, the juice of the 9 fruits was pooled into a single composite sample and processed jointly. Fruits were squeezed, and the juice was filtered to measure TSS (total soluble solids) and TA (titratable acidity). Fruit fractions were separated, weighed, and expressed in the forms of juice, peel, and

pulp percentages. The TSS of the juice was measured at 25 °C with a digital refractometer (Model Palette PR-100, Atago Co., Ltd., Tokyo, Japan) and TA (expressed as the percentage of citric acid in the juice) was determined by titration with 0.1 N NaOH to pH 8.1, using an automatic titrator (CRISON TitroMatic 2S, Crison Instruments S.A., Barcelona, Spain). Maturity index (MI) was expressed as the  $TSS \times 10/TA$  ratio.

### 2.3. Statistical Analysis

All data were first checked for outliers and for compliance with normality and homogeneity of variances using Shapiro–Wilk and Levene tests, respectively. When necessary, variables were log- or square-root-transformed before analysis to improve normality; untransformed means are presented for clarity.

The experimental unit was the individual tree. For variables measured once per tree and year (soil chemical properties, soil microbiology and nematodes, leaf mineral composition, yield components, pruning weight, and fruit quality), data were analyzed within a linear mixed-model framework, with treatment (Control vs. OXY), year, and their interaction as fixed effects and tree (nested within block) as a random factor. Repeated measurements across years on the same trees were modelled by specifying year as a repeated factor within tree, using a compound-symmetry covariance structure. When the treatment  $\times$  year interaction was not significant ( $p \geq 0.05$ ), it was removed from the final model and main effects were interpreted. Root biomass was assessed only once, at the end of the experimental period. Therefore, root dry weight data were analyzed using a one-way ANOVA with treatment as the fixed factor and tree as the experimental unit.

For time-series variables measured repeatedly within each season, such as dissolved O<sub>2</sub> in irrigation water (DO), soil O<sub>2</sub> diffusion rate (ODR), soil CO<sub>2</sub> and H<sub>2</sub>O vapor fluxes, midday stem water potential ( $\Psi_{stem}$ ), leaf gas exchange ( $A_{CO_2}$ ,  $g_s$ ,  $E_{leaf}$ ), and intrinsic and instantaneous leaf water use efficiency ( $A_{CO_2}/g_s$  and  $A_{CO_2}/E_{leaf}$ ), factorial repeated-measures ANOVA was performed in a mixed-model framework, with treatment as the between-subject factor and day of year (DOY) as the within-subject (repeated) factor, using the individual tree as the random subject. This approach explicitly accounted for the temporal correlation of observations within each tree. For these models, we tested the main effects of treatment and DOY and their interaction (treatment  $\times$  DOY).

When a significant interaction was detected ( $p < 0.05$ ), simple effects were explored and pairwise comparisons between treatments at a given year or sampling date were carried out using Duncan's multiple range test at  $p < 0.05$ . In all figures,  $p$ -values for treatment, time, and their interaction from the repeated-measures analyses are shown, together with standard errors (SEs). Additionally, we performed a post hoc power analysis for orchard-scale yield differences ( $\alpha = 0.05$ , two-tailed;  $n = 12$  trees per treatment/year).

All statistical analyses were performed using Statgraphics Centurion XV, version 15.2.06 (StatPoint Technologies Inc., Warrenton, VA, USA).

## 3. Results

### 3.1. Climatic Conditions and Irrigation Water Applied During the Experimental Period

During the experimental period (2018–2021), reference evapotranspiration (ET<sub>0</sub>) ranged from 1138 to 1246 mm, showing a low inter-annual variability. In contrast, annual rainfall (R) exhibited substantial year-to-year variation, with the lowest value recorded in 2018 (304 mm) and the highest in 2019 (512 mm) (Table 1), mainly due to torrential rains that occurred in September (255 mm in four days) (Figure 1).

**Table 1.** Reference evapotranspiration ( $ET_0$ ), rainfall (R), and irrigation water applied for each treatment during experimental period (2018–2022).

Seasons	$ET_0$ (mm)	R (mm)	Irrigation Treatments (mm)	
2018	1246	304	Control	588
2019	1192	512	OXY	548
2020	1160	334	547	539
2021	1138	385	538	470
Average 2018–2021	1184	384	536	526

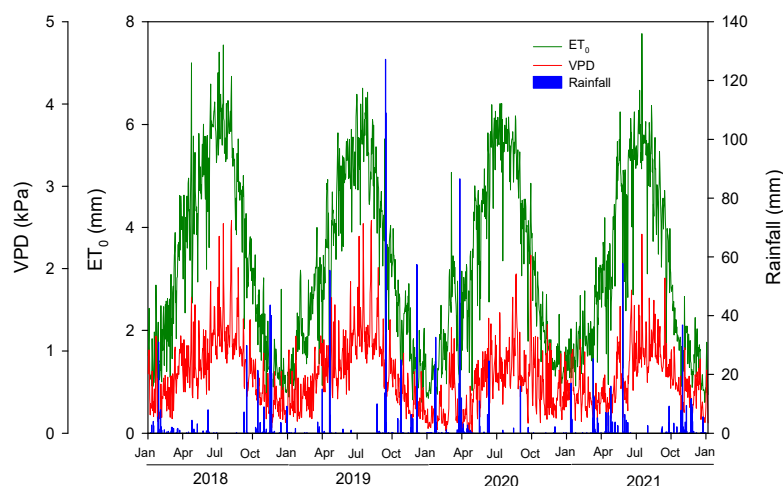


**Figure 1.** Seasonal evolution of daily vapor pressure deficit (VPD), reference evapotranspiration ( $ET_0$ ), and rainfall during the experimental period (2018 to 2021).

The seasonal change in the air vapor pressure deficit (VPD), reference evapotranspiration ( $ET_0$ ), and rainfall during the 2018–2021 seasons showed a clear seasonal pattern typical of Mediterranean conditions (Figure 1). Both VPD and  $ET_0$  exhibited marked increases from spring to early autumn, coinciding with the period of highest evaporative demand. Maximum  $ET_0$  values reached  $7.7 \text{ mm day}^{-1}$  in July 2021 while the maximum VPD reached a value of  $2.59 \text{ kPa}$  in mid-summer (August 2019).

Rainfall events (blue bars in Figure 1) were mainly concentrated during the autumn and winter, with scarce precipitation during the summer months. The most pronounced rainfall episodes were recorded in late 2018 and September 2019, whereas 2020 and 2021 showed lower and more irregular distributions. Overall, the climatic pattern revealed strong intra-annual variability in atmospheric water demand, characterized by extended periods of high VPD and  $ET_0$  coupled with limited rainfall.

Irrigation volumes were adjusted according to climatic demand in both treatments. In the Control treatment, the applied irrigation ranged from  $470 \text{ mm}$  (2021) to  $588 \text{ mm}$  (2018), while in the OXY treatment, the values were similar, ranging from  $470 \text{ mm}$  to  $548 \text{ mm}$  (Table 1). The differences in the amount of water applied between treatments in 2018 (around 7% less in OXY) were caused by temporary dripper blockages due to biofilm cleaning accumulated in secondary pipes at the beginning of  $\text{H}_2\text{O}_2$  application. The highest irrigation requirement occurred in 2018, corresponding to relatively low rainfall ( $304 \text{ mm}$ ) and high  $ET_0$  ( $1246 \text{ mm}$ ), while the lowest was observed in 2021, coinciding with a low  $ET_0$  ( $1138 \text{ mm}$ ) and a relatively high rainfall ( $385 \text{ mm}$ ). Across all seasons, irrigation inputs remained similar between treatments, ensuring comparable water availability for the experimental design.

### 3.2. Effects of Oxyfertigation on Soil

#### 3.2.1. Dissolved Oxygen in Irrigation Water and Soil Oxygen Diffusion Rate

The oxyfertigation treatment consistently increased dissolved oxygen (DO) in the irrigation water during both 2020 and 2021 (Figure 2A,C). The factorial repeated-measures ANOVA showed a significant treatment effect and strong temporal variability across sampling days. Importantly, a significant treatment  $\times$  DOY interaction was detected in both seasons, indicating that DO enhancement by oxyfertigation was not constant over time but varied according to environmental conditions, irrigation events, and water temperature. On multiple dates, post hoc Duncan comparisons confirmed significant differences between treatments ( $p < 0.05$ ), particularly during periods of high evaporative demand or elevated seasonal water temperature. In 2020, DO in the Control treatment ranged between 2.7 and 7.8 mg L<sup>-1</sup> (mean = 5.0 mg L<sup>-1</sup>), whereas in the OXY treatment, it varied from 18.4 to 31.4 mg L<sup>-1</sup> (mean = 22.7 mg L<sup>-1</sup>). Oxygen-enriched water consistently maintained DO levels approximately four times higher than Control across all sampling dates. During the 2021 period, a similar trend was recorded. Control treatment showed values between 3.7 and 8.0 mg L<sup>-1</sup> (mean = 5.5 mg L<sup>-1</sup>) while the OXY treatment presented concentrations from 16.0 to 49.7 mg L<sup>-1</sup> (mean = 29.3 mg L<sup>-1</sup>).

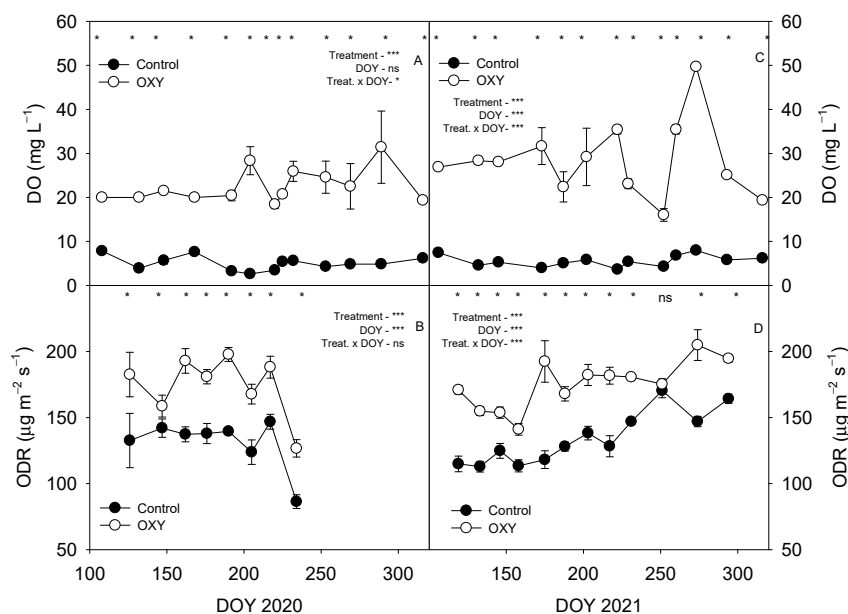


**Figure 2.** Seasonal evolution of dissolved O<sub>2</sub> (DO) concentration in the irrigation water measured at the dripper and soil O<sub>2</sub> diffusion rate (ODR) and for each treatment (Control and OXY) during the 2020 (A,B) and 2021 (C,D) periods. Each point is the average of 4 measurements of DO in irrigation water measured in the dripper and 12 measurements in soil ODR. Vertical bars indicate  $\pm$  standard error. The  $p$ -values corresponding to the effects of treatment, day of year (DOY), and their interaction (treatment  $\times$  DOY) obtained from factorial repeated-measures ANOVA, in a mixed-model framework, are shown inside each panel. The symbols ns, \*, and \*\*\* denote non-significant differences,  $p < 0.05$ , and  $p < 0.001$ , respectively. Asterisks above individual dates indicate significant differences between treatments on a given sampling date according to Duncan's test ( $p < 0.05$ ).

Soil oxygen diffusion rate (ODR) also increased systematically under oxyfertigation during 2020 and 2021 (Figure 2B,D). Treatment and day effects were significant ( $p < 0.001$ ), reflecting both improved rhizosphere aeration and the expected temporal sensitivity of ODR to irrigation cycles and meteorological conditions. The treatment  $\times$  DOY interaction was non-significant in 2020 but became significant in 2021, suggesting that temporal divergence between treatments was more pronounced during the latter season, when

increased soil temperature and irrigation intensity may have amplified the oxygenation response. As with DO, isolated dates showed pairwise differences ( $p < 0.05$ ), confirming the episodic enhancement of root-zone aeration under oxyfertigation. The soil ODR under oxyfertigation consistently exhibited higher values ( $150\text{--}200 \mu\text{g O}_2 \text{ m}^{-2} \text{ s}^{-1}$ ) than Control ( $100\text{--}150 \mu\text{g O}_2 \text{ m}^{-2} \text{ s}^{-1}$ ).

Collectively, these results demonstrate that oxyfertigation not only increased the baseline levels of oxygen supply to the root environment but also modulated temporal aeration dynamics in response to changing environmental conditions, with variable interaction effects across years.

### 3.2.2. Soil Respiration

Seasonal patterns of soil  $\text{CO}_2$  fluxes showed a gradual decline from spring to late summer under both treatments in 2020 (Figure 3A) and 2021 (Figure 3B). Across both years, the repeated-measures analysis revealed a significant effect of sampling day ( $p < 0.001$ ), reflecting seasonal dynamics, while treatment effects remained non-significant. No treatment  $\times$  DOY interaction was detected, indicating that both treatments followed comparable temporal trajectories. In 2020, isolated dates exhibited small but significant differences between treatments, with higher  $\text{CO}_2$  fluxes under OXY (Figure 3A), although these differences were not repeated later in the season or in 2021.

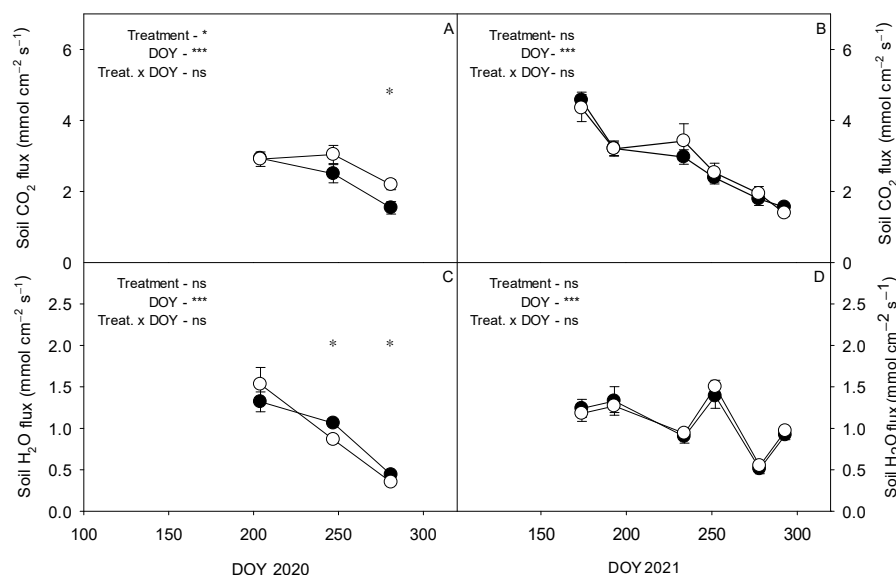


**Figure 3.** Seasonal evolution of soil  $\text{CO}_2$  and  $\text{H}_2\text{O}$  vapor fluxes ( $\text{mmol cm}^{-2} \text{ s}^{-1}$ ) under Control and OXY treatments in 2020 (A,C) and 2021 (B,D). Closed circles connected by solid lines represent the Control treatment and open circles connected by solid lines represent the OXY treatment. Each point represents the mean of 12 measurements per treatment and sampling date (three trees per block, four blocks). Vertical bars indicate  $\pm$  standard error (SE). The  $p$ -values corresponding to the effects of treatment, day of year (DOY), and their interaction (treatment  $\times$  DOY), obtained from factorial repeated-measures ANOVA in a mixed-model framework, are shown within each panel. The symbols ns, \*, and \*\*\* denote non-significant differences,  $p < 0.05$ , and  $p < 0.001$ , respectively. Asterisks plotted at individual dates indicate significant differences between treatments on that date according to Duncan's test ( $p < 0.05$ ).

Soil  $\text{H}_2\text{O}$  vapor fluxes behaved similarly, decreasing progressively during the summer in 2020 (Figure 3C) and showing higher temporal variability in 2021 (Figure 3D). DOY effects were again highly significant ( $p < 0.001$ ) whereas neither treatment nor treatment  $\times$  DOY interaction significantly affected  $\text{H}_2\text{O}$  vapor emission. As with  $\text{CO}_2$  fluxes, occasional date-specific differences in 2020 favored the OXY treatment (Figure 3C), but these did not occur consistently in 2021.

Overall, soil CO<sub>2</sub> and H<sub>2</sub>O vapor emissions exhibited strong seasonal dependence linked to environmental conditions, without evidence of a systematic oxyfertigation effect across the entire monitoring period.

### 3.2.3. Soil Chemical Composition

Soil chemical properties, including salinity parameters, soil reaction, and organic matter, were evaluated under both treatments in 2020 and 2021 (Table 2). Across both years, the application of oxyfertigation did not alter the chemical composition or fertility of the soil during the study period as no statistically significant differences were observed between treatments in any of the measured variables. Moreover, the addition of H<sub>2</sub>O<sub>2</sub> to the irrigation water did not induce significant modifications in soil physicochemical properties under the tested conditions as both treatments maintained similar salinity levels and pH values (Table 2), as well as a stable organic matter content.

However, soil salinity, soil reaction, and organic matter parameters showed clear interannual variability, whereas no significant effects of the year  $\times$  treatment interactions were detected for any of the evaluated variables (Table 2). Exchangeable sodium was significantly affected by year, with higher values recorded in 2021 than in 2020. Soil pH showed a highly significant year effect, decreasing from moderately alkaline values in 2020 to slightly lower values in 2021, regardless of treatment. Active limestone was significantly affected by year, with higher values observed in 2021 compared with 2020. Organic matter and organic carbon also showed significant year effects, increasing from 2020 to 2021.

The detailed soil mineral composition, including primary and secondary macronutrients, micronutrients, and the cation exchange capacity (CEC), for the Control and OXY treatments during the 2020 and 2021 seasons is shown in Table 3. The OXY treatment maintained similar chemical characteristics and nutrient balance compared with the Control treatment as the OXY treatment did not significantly affect soil nutrient availability or exchange capacity in the short term throughout both years. No statistically significant differences were detected between treatments in any of the evaluated parameters (Table 3).

Most soil fertility parameters remained statistically stable between 2020 and 2021 (Table 3). Assimilable phosphorus was the only macronutrient significantly affected by year, with higher values recorded in 2020 than in 2021, under both treatments. Among the micronutrients, only assimilable boron showed a highly significant year effect, increasing markedly from 2020 to 2021. No significant effects of year  $\times$  treatment interactions were detected for any of the nutrients or for cation exchange capacity.

### 3.2.4. Soil Microbiology and Nematode Phytopathology

The results of soil microbiology and nematode phytopathology showed different responses depending on the factor considered (Table 4). Regarding nematode phytopathology, *Tylenchulus* spp. populations were significantly affected by treatment. However, the confidence intervals indicate that *Tylenchulus* spp. counts are highly variable among trees, particularly under the OXY treatment (Table S7 Supplementary Materials), which is reflected in very wide intervals and even negative lower limits (truncated to 0 for biological interpretation). Nevertheless, the overall analysis revealed significant differences between treatments in the mean number of nematodes. In 2020, *Tylenchulus* spp. density was substantially higher under the Control than under the OXY treatment. A similar tendency was observed in 2021. When both years were considered together, oxyfertigation was consistently associated with lower *Tylenchulus* spp. populations than Control.

Molds and yeasts were the only soil microbials studied that were significantly affected by year, with higher values recorded in 2021 than in 2020 under both treatments.

**Table 2.** Soil mineral content related to salinity, soil reaction, and organic matter in the 0–30 cm layer for each treatment (Control and OXY) during the last two seasons of the experiment (2020 and 2021). Values are means  $\pm$  standard error (SE,  $n = 4$  trees per treatment and year).

Year	Treatment	Salinity				Soil Reaction and Organic Matter					
		CE ( $\text{mS cm}^{-1}$ )	Chloride ( $\text{meq 100 g}^{-1}$ )	Sulfate (% p/p)	Exchange Sodium ( $\text{meq 100 g}^{-1}$ )	pH	Total Limestone (% p/p)	Active Limestone (% p/p)	Organic Matter (% p/p)	Organic Carbon (% p/p)	C/N
2020	Control	$0.36 \pm 0.01$	$0.33 \pm 0.02$	$0.04 \pm 0.01$	$0.31 \pm 0.03$	$7.95 \pm 0.09$	$30.20 \pm 3.55$	$10.93 \pm 1.31$	$1.98 \pm 0.19$	$1.15 \pm 0.11$	$6.73 \pm 0.35$
	OXY	$0.41 \pm 0.02$	$0.38 \pm 0.03$	$0.04 \pm 0.01$	$0.33 \pm 0.05$	$7.94 \pm 0.02$	$31.43 \pm 1.29$	$11.11 \pm 0.36$	$2.06 \pm 0.13$	$1.20 \pm 0.07$	$6.50 \pm 0.19$
2021	Control	$0.39 \pm 0.03$	$0.43 \pm 0.03$	$0.05 \pm 0.01$	$0.53 \pm 0.09$	$7.45 \pm 0.09$	$35.20 \pm 3.00$	$13.93 \pm 0.97$	$2.68 \pm 0.27$	$1.55 \pm 0.16$	$9.37 \pm 0.33$
	OXY	$0.34 \pm 0.07$	$0.34 \pm 0.11$	$0.04 \pm 0.01$	$0.52 \pm 0.11$	$7.31 \pm 0.05$	$35.23 \pm 2.45$	$13.25 \pm 0.59$	$2.35 \pm 0.26$	$1.36 \pm 0.15$	$8.97 \pm 0.19$
ANOVA											
Treatment		ns	ns	ns	ns	ns	ns	ns	ns	ns	ns
Year		ns	ns	ns	*	***	ns	*	*	*	ns
Treatment $\times$ Year		ns	ns	ns	ns	ns	ns	ns	ns	ns	ns

ns, \*, and \*\*\* indicate non-significant differences,  $p < 0.05$ , and  $p < 0.001$ , respectively.  $p$ -values correspond to the effects of treatment, year, and their interaction obtained from factorial repeated-measures ANOVA in a mixed-model framework.

**Table 3.** Soil mineral nutrients (primary and secondary macronutrients, micronutrients, and cation exchange capacity) in the 0–30 cm layer for each treatment (Control and OXY) during the last two seasons of the experiment (2020 and 2021). Values are means  $\pm$  standard error (SE,  $n = 4$  trees per treatment and year).

Year	Treatment	Primary Macronutrients				Secondary Macronutrients			Micronutrients	Cation Exchange Capacity
		Total Nitrogen (% p/p)	Soluble Nitric Nitrogen ( $\text{mg kg}^{-1}$ )	Soluble Nitrate ( $\text{mg kg}^{-1}$ )	Assimilable Phosphorous ( $\text{mg kg}^{-1}$ )	Exchange Potassium ( $\text{meq 100 g}^{-1}$ )	Exchange Calcium ( $\text{meq 100 g}^{-1}$ )	Exchange Magnesium ( $\text{meq 100 g}^{-1}$ )	Assimilable Boron ( $\text{mg kg}^{-1}$ )	C.I.C. ( $\text{meq 100 g}^{-1}$ )
2020	Control	$0.17 \pm 0.01$	$22.23 \pm 1.98$	$98.6 \pm 8.9$	$148.3 \pm 16.4$	$0.94 \pm 0.07$	$8.80 \pm 0.28$	$3.21 \pm 0.22$	$0.19 \pm 0.02$	$13.30 \pm 0.57$
	OXY	$0.18 \pm 0.01$	$22.66 \pm 2.93$	$100.3 \pm 13.1$	$156.3 \pm 6.8$	$1.08 \pm 0.09$	$9.67 \pm 0.59$	$2.82 \pm 0.41$	$0.24 \pm 0.01$	$13.93 \pm 1.13$
2021	Control	$0.17 \pm 0.01$	$40.00 \pm 5.03$	$177.0 \pm 22.3$	$121.3 \pm 14.7$	$1.09 \pm 0.08$	$10.13 \pm 0.74$	$3.89 \pm 0.49$	$0.71 \pm 0.06$	$15.67 \pm 1.35$
	OXY	$0.15 \pm 0.02$	$32.13 \pm 13.74$	$142.0 \pm 60.7$	$125.3 \pm 8.7$	$1.05 \pm 0.20$	$10.40 \pm 0.77$	$3.79 \pm 0.45$	$0.67 \pm 0.09$	$15.77 \pm 1.53$
ANOVA										
Treatment		ns	ns	ns	ns	ns	ns	ns	ns	ns
Year		ns	ns	ns	*	ns	ns	ns	***	ns
Treatment $\times$ Year		ns	ns	ns	ns	ns	ns	ns	ns	ns

ns, \*, and \*\*\* indicate non-significant differences,  $p < 0.05$ , and  $p < 0.001$ , respectively.  $p$ -values correspond to the effects of treatment, year, and their interaction obtained from factorial repeated-measures ANOVA in a mixed-model framework.

**Table 4.** Soil microbiology and nematode phytopathology in the 0–30 cm layer for each treatment (Control and OXY) during the last two seasons of the experiment (2020 and 2021). Values are means  $\pm$  standard error (SE,  $n = 4$  trees per treatment and year).

Year	Treatment	Soil Microbiology			Nematode Phytopathology	
		Aerobic Mesophilic ( $\text{ufc g}^{-1}$ )	Molds and Yeasts ( $\text{ufc g}^{-1}$ )	Actinomycetes ( $\text{ufc g}^{-1}$ )	<i>Tylenchulus</i> spp. (Nematode $100 \text{ g}^{-1}$ )	Saprophytic Soil Nematodes (Nematode $100 \text{ g}^{-1}$ )
2020	Control	17,733,333 $\pm$ 3,055,050	44,000 $\pm$ 5508	106,667 $\pm$ 3333	2144.7 $\pm$ 146.5	174.0 $\pm$ 37.7
	OXY	21,000,000 $\pm$ 5,544,166	57,000 $\pm$ 15,000	126,667 $\pm$ 3333	719.7 $\pm$ 607.0	101.7 $\pm$ 126.2
2021	Control	28,000,000 $\pm$ 3,333,333	130,000 $\pm$ 577	456,667 $\pm$ 577	931.0 $\pm$ 227.4	107.0 $\pm$ 21.9
	OXY	24,666,667 $\pm$ 9,848,858	95,000 $\pm$ 10,000	226,667 $\pm$ 10,000	574.0 $\pm$ 547.4	67.7 $\pm$ 35.2
ANOVA						
Treatment		ns	ns	ns	*	ns
Year		ns	***	ns	ns	ns
Treatment $\times$ Year		ns	ns	ns	ns	ns

ns, \*, and \*\*\* indicate non-significant differences,  $p < 0.05$ , and  $p < 0.001$ , respectively.  $p$ -values correspond to the effects of treatment, year, and their interaction obtained from factorial repeated-measures ANOVA in a mixed-model framework.

### 3.3. Effects of Oxyfertigation in the Plant

#### 3.3.1. Plant Water Relations and Leaf Gas Exchange

During the experimental period (2018–2021), the seasonal change in midday stem water potential ( $\Psi_{\text{stem}}$ ) displayed strong seasonal dynamics driven by environmental conditions, particularly rainfall events and evaporative demand (Figure 4A–D). The factorial repeated-measures ANOVA revealed highly significant day effects across all seasons, indicating marked temporal autocorrelation and reflecting physiological adjustments to changing atmospheric and soil conditions. Treatment effects were generally non-significant across years, and a non-significant treatment  $\times$  DOY interaction was detected during 2019, 2020, or 2021. This demonstrates that both irrigation strategies followed similar temporal trajectories and that oxyfertigation did not systematically modify  $\Psi_{\text{stem}}$  under these field conditions. However, in 2018, a significant treatment  $\times$  DOY interaction was detected, indicating that oxyfertigation transiently affected  $\Psi_{\text{stem}}$  at specific sampling dates within that season. On those isolated days, oxyfertigated trees showed a slightly less negative water potential than control trees, suggesting reduced midday stress. Nonetheless, the magnitude and duration of these differences were episodic and did not persist across subsequent seasons. Isolated comparisons at individual dates in 2021 also showed occasional significant differences between treatments, but these were not systematic and did not produce a consistent seasonal shift. Overall, short-term divergences between treatments were rare and transient, and they did not accumulate into a year-level effect.

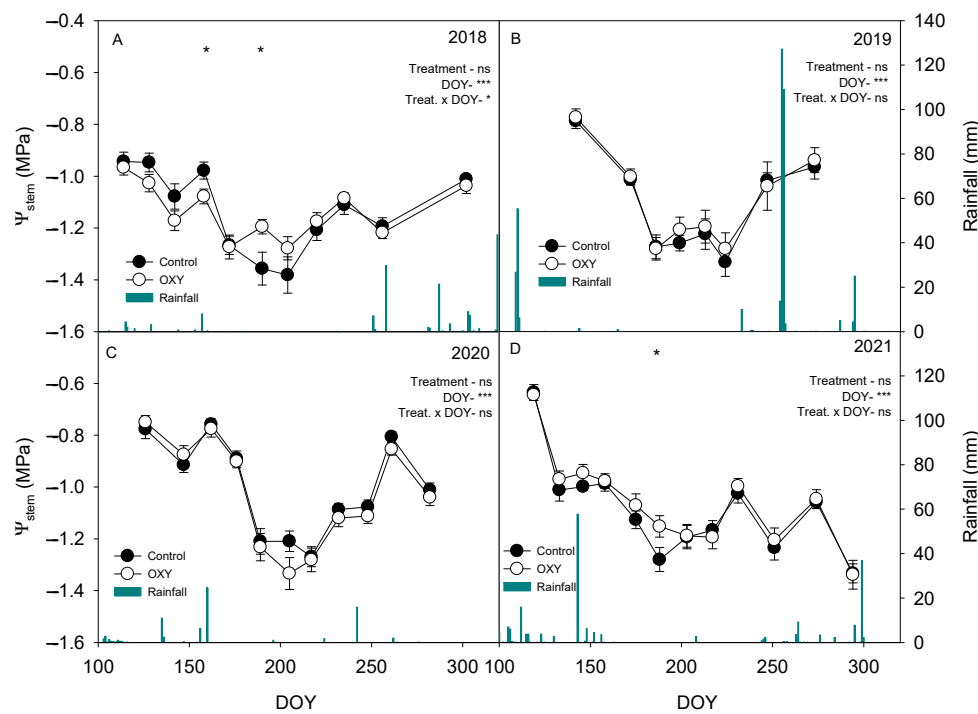


**Figure 4.** Seasonal evolution of midday stem water potential ( $\Psi_{\text{stem}}$ ) and rainfall (A–D) for each treatment (Control and OXY) during the experimental period (2018 to 2021). Symbols represent the mean  $\Psi_{\text{stem}}$  of 12 trees per treatment and sampling date; vertical bars indicate  $\pm$  standard error (SE). The  $p$ -values corresponding to the effects of treatment, day of year (DOY), and their interaction (treatment  $\times$  DOY), obtained from factorial repeated-measures ANOVA in a mixed-model framework, are given within each panel. The symbols ns, \*, and \*\*\* denote non-significant differences,  $p < 0.05$ , and  $p < 0.001$ , respectively. Asterisks plotted at individual dates indicate significant differences between treatments on that date according to Duncan's test ( $p < 0.05$ ).

Throughout the 2018–2021 seasons, leaf gas exchange variables showed pronounced seasonal variation, driven mainly by climatic conditions and crop phenology (Figure 5). The repeated-measures ANOVA revealed highly significant day effects for all variables, confirming strong temporal dependence associated with changing atmospheric demand.

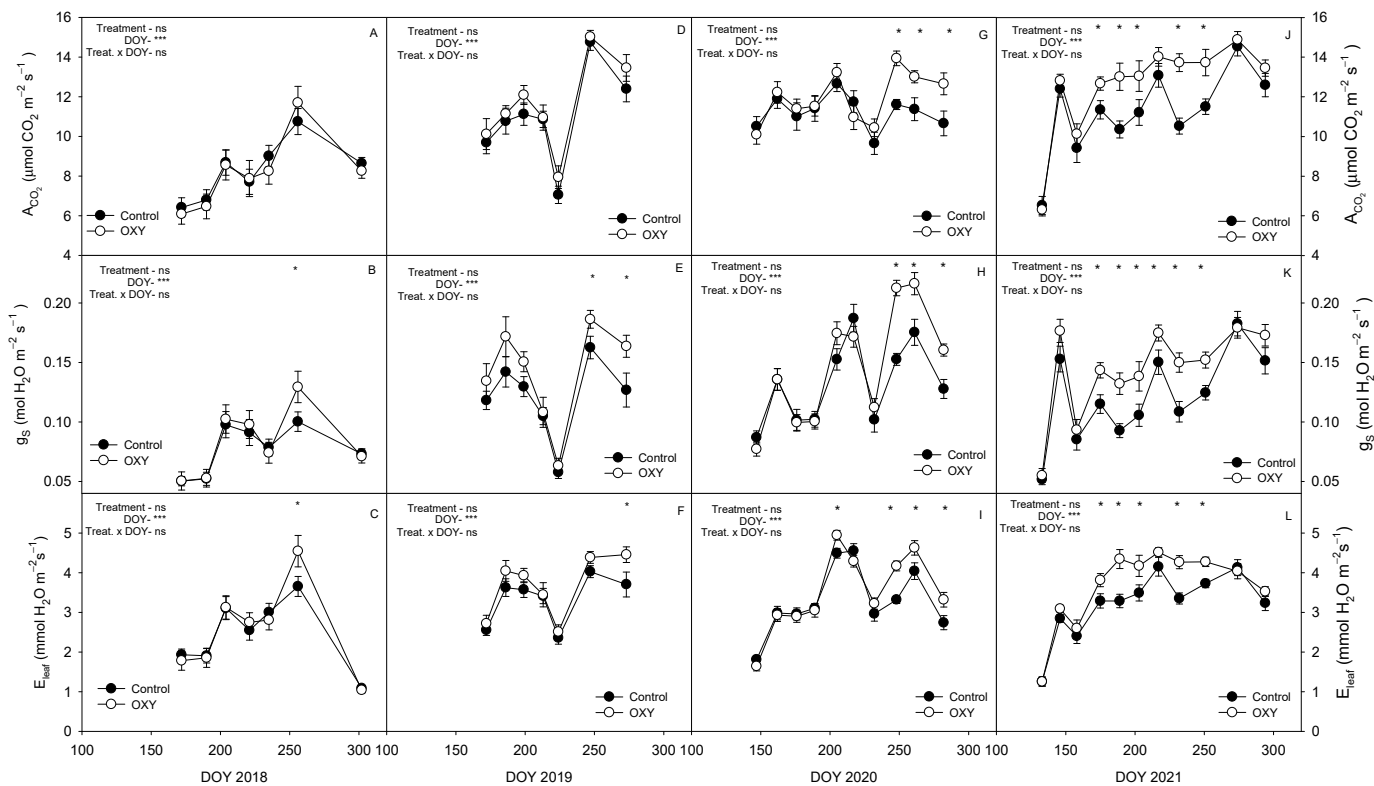


**Figure 5.** Seasonal change in leaf  $\text{CO}_2$  assimilation rate ( $A_{\text{CO}_2}$ ,  $\mu\text{mol CO}_2 \text{ m}^{-2} \text{ s}^{-1}$ ), stomatal conductance ( $g_s$ ,  $\text{mol H}_2\text{O m}^{-2} \text{ s}^{-1}$ ), and transpiration rate ( $E_{\text{leaf}}$ ,  $\text{mmol H}_2\text{O m}^{-2} \text{ s}^{-1}$ ) for each treatment (Control and OXY) during the 2018 (A–C), 2019 (D–F), 2020 (G–I), and 2021 (J–L) seasons. Each symbol represents the mean of 12 measurements per treatment and sampling date. Vertical bars indicate  $\pm$  standard error (SE). The  $p$ -values corresponding to the effects of treatment, day of year (DOY), and their interaction (treatment  $\times$  DOY), obtained from factorial repeated-measures ANOVA in a mixed-model framework, are shown within each panel. The symbols ns, and \*\*\* denote non-significant differences, and  $p < 0.001$ , respectively. Asterisks plotted at individual dates indicate significant differences between treatments on that date according to Duncan's test ( $p < 0.05$ ).

Treatment effects on  $A_{\text{CO}_2}$ ,  $g_s$ , and  $E_{\text{leaf}}$  were not statistically significant at the seasonal scale, and no treatment  $\times$  day interaction was detected for most years, indicating that oxyfertigation did not systematically modify leaf-level gas exchange dynamics under field conditions. Nevertheless, isolated differences between treatments were detected at specific sampling dates, particularly during high evaporative demand, with oxyfertigated trees often showing slightly higher  $A_{\text{CO}_2}$ ,  $g_s$  and  $E_{\text{leaf}}$  than the control. However, these point-level contrasts did not accumulate into a consistent treatment effect when evaluated across the crop cycle.

Seasonal variation in intrinsic leaf water use efficiency ( $A_{\text{CO}_2}/g_s$ ) showed marked temporal dynamics across all growing seasons (Figure 6A,C,E,G). The repeated-measures ANOVA indicated a strong day effect whereas treatment effects remained non-significant, with no sustained treatment  $\times$  DOY. Transient differences between treatments were detected only at isolated sampling dates, particularly under peak evaporative demand, but these did not persist across years. Instantaneous leaf water use efficiency ( $A_{\text{CO}_2}/E_{\text{leaf}}$ ) also displayed high temporal variability at the beginning of each season and progressively

stabilized during mid-season (Figure 6B,D,F,H). The day effect was significant, confirming the strong environmental control on leaf-level WUE (water use efficiency), while neither treatment nor treatment  $\times$  DOY interaction effects were significant. Occasional point differences were observed under specific conditions but were not recurrent across seasons. In general, oxyfertigation did not induce a sustained improvement in  $A_{CO_2}/g_s$  or  $A_{CO_2}/E_{leaf}$  at the leaf scale. Seasonal trajectories were primarily driven by atmospheric demand and water availability, indicating that any physiological benefits associated with improved root aeration were episodic and context-dependent rather than consistent over time.

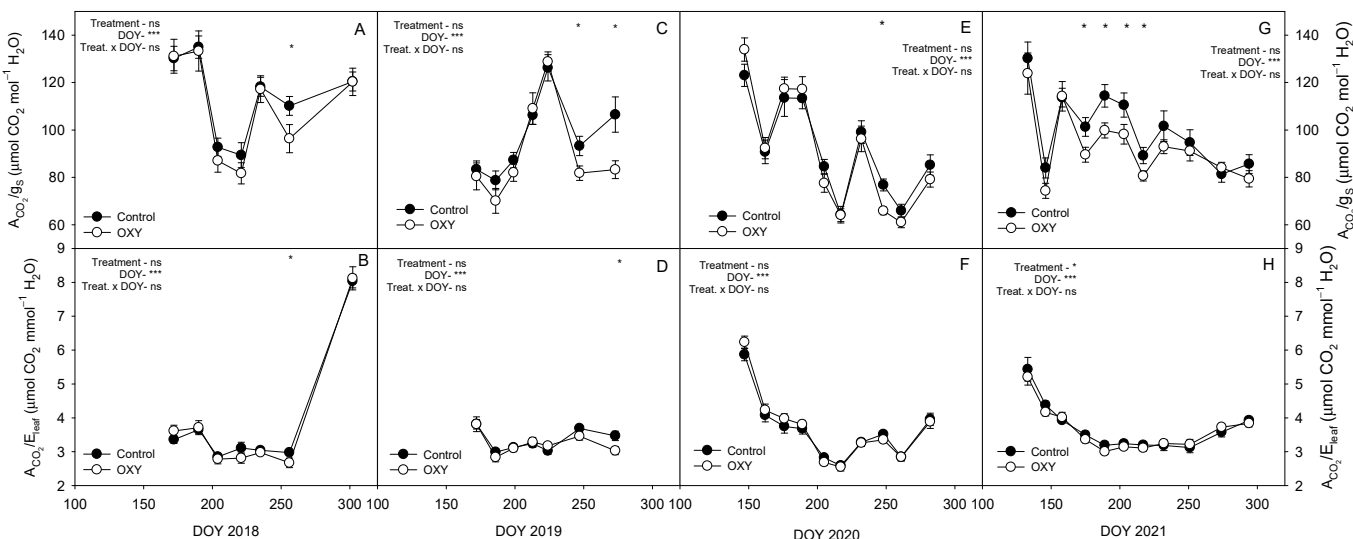


**Figure 6.** Seasonal evolution of intrinsic leaf water use efficiency ( $A_{CO_2}/g_s$ ,  $\mu\text{mol CO}_2 \text{ mol}^{-1} \text{ H}_2\text{O}$ ) and instantaneous leaf water use efficiency ( $A_{CO_2}/E_{leaf}$ ,  $\mu\text{mol CO}_2 \text{ mmol}^{-1} \text{ H}_2\text{O}$ ) and for each treatment (Control and OXY) during 2018 (A,B), 2019 (C,D), 2020 (E,F), and 2021 (G,H). Each symbol represents the mean of 12 measurements per treatment and sampling date. Vertical bars indicate  $\pm$  standard error (SE). The  $p$ -values corresponding to the effects of treatment, day of year (DOY), and their interaction (treatment  $\times$  DOY), obtained from factorial repeated-measures ANOVA in a mixed-model framework, are shown within each panel. The symbols ns, \* and \*\*\* denote non-significant differences,  $p < 0.05$  and  $p < 0.001$ , respectively. Asterisks plotted at individual dates indicate significant differences between treatments on that date according to Duncan's test ( $p < 0.05$ ).

### 3.3.2. Crop Growth

The absolute growth rate of the trunk cross-sectional area ( $AGR_{Trunk}$ ) showed a clear interannual decline over the experimental period, with highly significant year effects but no significant treatment effect or treatment  $\times$  year interaction (Table 5). Mean  $AGR_{Trunk}$  values were similar between treatments within each season, and accumulated trunk growth over 2018–2021 did not differ appreciably between Control and OXY.

In contrast, fresh pruning weight was significantly affected by both year ( $p < 0.001$ ) and treatment ( $p < 0.05$ ), with no significant treatment  $\times$  year interaction. From 2019 onwards, OXY trees consistently exhibited higher pruning biomass than Control trees, particularly in 2020, when pruning weight reached  $18.0 \pm 1.50 \text{ kg tree}^{-1}$  in OXY compared with  $14.0 \pm 1.58 \text{ kg tree}^{-1}$  in Control. Over the 2019–2021 period, accumulated pruning weight was greater under OXY ( $39.8 \pm 3.04 \text{ kg tree}^{-1}$ ) than under Control ( $33.2 \pm 2.43 \text{ kg tree}^{-1}$ ), indicating a sustained stimulation of vegetative growth under oxyfertigation.

**Table 5.** Absolute growth rate of the trunk cross-sectional area ( $AGR_{Trunk}$ ,  $\text{cm}^2 \text{ year}^{-1}$ ) and fresh pruning weight ( $\text{kg tree}^{-1}$ ) for each treatment (Control and OXY) during the experimental period (2018–2021). Values are means  $\pm$  standard error (SE,  $n = 12$  trees per treatment and year).

Year	Treatment	$AGR_{Trunk}$ ( $\text{cm}^2 \text{ Year}^{-1}$ )	Fresh Pruning Weight ( $\text{kg Tree}^{-1}$ )
2018	Control	$10.1 \pm 1.10$	-
	OXY	$7.8 \pm 1.52$	-
2019	Control	$10.2 \pm 1.24$	$12.2 \pm 0.91$
	OXY	$11.5 \pm 2.12$	$14.6 \pm 1.58$
2020	Control	$7.6 \pm 0.99$	$14.0 \pm 1.58$
	OXY	$8.5 \pm 1.52$	$18.0 \pm 1.50$
2021	Control	$4.4 \pm 0.52$	$7.1 \pm 0.82$
	OXY	$6.3 \pm 0.93$	$7.2 \pm 0.70$
		<b>2018–2021</b>	<b>2019–2021</b>
Accumulated	Control	$22.2 \pm 2.40$	$33.2 \pm 2.43$
	OXY	$22.5 \pm 3.16$	$39.8 \pm 3.04$
ANOVA			
Treatment		ns	*
Year		***	***
Treatment $\times$ Year		ns	ns

ns, \*, and \*\*\* indicate non-significant differences,  $p < 0.05$ , and  $p < 0.001$ , respectively.  $p$ -values correspond to the effects of treatment, year, and their interaction obtained from factorial repeated-measures ANOVA in a mixed-model framework. Accumulated values are presented for descriptive purposes and were not included in the ANOVA.

### 3.3.3. Root Biomass Distribution

At the end of the experimental period (November 2021), no statistically significant differences were detected between treatments for root dry weight at any soil depth or root fraction (Table 6). Fine root biomass values in the surface layer (0–15 cm) were similar between treatments, averaging  $0.67 \times 10^2 \text{ g cm}^{-3}$  in Control and  $0.65 \times 10^2 \text{ g cm}^{-3}$  under OXY. In contrast, thick root biomass in this layer showed a slight, non-significant increase in the OXY treatment ( $0.22 \times 10^2 \text{ g cm}^{-3}$  vs.  $0.13 \times 10^2 \text{ g cm}^{-3}$ ). In the deeper layer (15–30 cm), oxyfertigated trees exhibited greater root accumulation, particularly in the thick root fraction ( $1.64 \times 10^2 \text{ g cm}^{-3}$  vs.  $0.10 \times 10^2 \text{ g cm}^{-3}$  in Control) although variability prevented statistical significance. Overall, the total root biomass tended to be greater in oxyfertigated trees ( $2.87 \times 10^2 \text{ g cm}^{-3}$ ) than in Control ( $1.20 \times 10^2 \text{ g cm}^{-3}$ ), suggesting a positive but non-significant trend associated with  $\text{H}_2\text{O}_2$  enriched irrigation water, due to the strong dispersion of the data (Table S7 Supplementary Materials).

**Table 6.** Root dry weight ( $\times 10^2 \text{ g cm}^{-3}$ ) of fine and thick roots at two soil depths for each treatment (Control and OXY) at the end of the experimental period (November 2021). Values are means  $\pm$  standard error (SE,  $n = 4$  trees per treatment).

2021	Fine 0–15 cm	Thick 0–15 cm	Total 0–15 cm	Fine 15–30 cm	Thick 15–30 cm	Total 15–30 cm	Total Fine	Total Thick	Total
Control	$0.67 \pm 0.14$	$0.13 \pm 0.07$	$0.80 \pm 0.15$	$0.30 \pm 0.08$	$0.10 \pm 0.08$	$0.39 \pm 0.12$	$0.97 \pm 0.15$	$0.23 \pm 0.11$	$1.20 \pm 0.04$
OXY	$0.65 \pm 0.17$	$0.22 \pm 0.11$	$0.86 \pm 0.12$	$0.37 \pm 0.15$	$1.64 \pm 1.44$	$2.01 \pm 1.39$	$1.02 \pm 0.32$	$1.86 \pm 1.55$	$2.87 \pm 1.39$
ANOVA	ns	ns	ns	ns	ns	ns	ns	ns	ns

ANOVA (one-way, treatment effect): ns for all variables. ‘ns’ indicates not significant differences at  $p < 0.05$ .

### 3.3.4. Leaf Mineral Nutrition

Across the four years, very few significant differences were detected between treatments for most macro- and micronutrients, indicating that oxyfertigation did not markedly alter leaf mineral composition (Table 7). Only Mg content was consistently lower under the OXY treatment than under the Control whereas the remaining nutrients remained statistically similar between treatments. In general, although oxyfertigation modified Mg concentration, its net impact on the nutritional status of citrus was limited under the studied conditions.

However, the leaf mineral composition of ‘Ortanique’ mandarin trees showed a marked interannual variability for most macro- and micronutrients (Table 7). Leaf N, P, and Mg contents were significantly affected by year, with values fluctuating across seasons. Sodium showed a significant year effect, with higher concentrations in 2018 and lower values in subsequent years, independently of treatment. All evaluated micronutrients (Fe, Cu, Mn, Zn, and B) were significantly affected by year, with values fluctuating across seasons. No significant treatment effects or year  $\times$  treatment interactions were detected for any of the macro- or micronutrients.

### 3.3.5. Yield

The effect of adding  $\text{H}_2\text{O}_2$  to the irrigation water on the yield parameters of ‘Ortanique’ mandarin trees was evaluated during the 2018–2021 experimental period (Table 8). Fruit yield showed marked interannual variability, with a highly significant year effect ( $p < 0.001$ ) but no significant treatment or treatment  $\times$  year interaction. In all four seasons, OXY trees exhibited numerically higher yields than Control trees, although these differences did not reach statistical significance; cumulative yield over 2018–2021 increased from  $289.1 \pm 27.3 \text{ kg tree}^{-1}$  in Control to  $326.2 \pm 26.1 \text{ kg tree}^{-1}$  under OXY.

In contrast, fruit load and crop water use efficiency (YWUE) were significantly affected by both treatment and year ( $p < 0.05$  and  $p < 0.001$ , respectively), with no significant treatment  $\times$  year interaction. OXY trees consistently produced more fruits per tree than Control trees from 2019 onwards, leading to a higher cumulative fruit number in OXY ( $2030 \pm 178 \text{ fruit tree}^{-1}$ ) compared with Control ( $1725 \pm 174 \text{ fruit tree}^{-1}$ ) over the four years. Mean fruit weight decreased progressively over time in both treatments, with a strong year effect ( $p < 0.001$ ) but no treatment effect, indicating a compensatory trade-off between fruit number and size. YWUE followed a similar pattern to yield, with significantly higher values under OXY in all years, resulting in an increase from  $11.2 \pm 1.06$  to  $12.9 \pm 1.03 \text{ kg m}^{-3}$  in the multi-year means, thus confirming a consistent improvement in water productivity under oxyfertigation. When cumulative production over the four-year period was considered, cumulative yield increased by approximately 13% and the total fruit number by about 18% under oxyfertigation. Effect sizes (Hedges'  $g$ ) for the yield, fruit number, mean fruit weight, and YWUE, by year and accumulated, are presented in Figure S1. The corresponding Cohen's  $d$ /Hedges'  $g$  numerical values are provided in Supplementary Table S13.

**Table 7.** Leaf mineral composition (primary and secondary macronutrients and microelements) of ‘Ortanique’ mandarin trees for each treatment (Control and OXY) during the experimental period (2018–2021). Values are means  $\pm$  standard error (SE,  $n = 12$  trees per treatment and year).

Year	Treatment	Primary Macronutrients			Secondary Macronutrients			Microelements				
		N (%)	P (%)	K (%)	Ca (%)	Mg (%)	Na (%)	Fe (ppm)	Cu (ppm)	Mn (ppm)	Zn (ppm)	B (ppm)
2018	Control	2.61 $\pm$ 0.12	0.147 $\pm$ 0.004	0.33 $\pm$ 0.02	4.49 $\pm$ 0.14	0.62 $\pm$ 0.01	0.18 $\pm$ 0.02	79 $\pm$ 2.2	16 $\pm$ 1.6	35 $\pm$ 2.1	34 $\pm$ 2.6	271 $\pm$ 13
	OXY	2.62 $\pm$ 0.14	0.149 $\pm$ 0.004	0.36 $\pm$ 0.03	4.22 $\pm$ 0.20	0.60 $\pm$ 0.02	0.24 $\pm$ 0.04	84 $\pm$ 5.8	18 $\pm$ 2.2	38 $\pm$ 1.9	37 $\pm$ 4.1	272 $\pm$ 11
2019	Control	2.77 $\pm$ 0.04	0.128 $\pm$ 0.004	0.35 $\pm$ 0.03	4.24 $\pm$ 0.15	0.52 $\pm$ 0.01	0.13 $\pm$ 0.01	65 $\pm$ 2.0	23 $\pm$ 1.7	23 $\pm$ 2.2	19 $\pm$ 1.0	275 $\pm$ 9
	OXY	2.87 $\pm$ 0.02	0.129 $\pm$ 0.003	0.44 $\pm$ 0.04	4.28 $\pm$ 0.13	0.50 $\pm$ 0.02	0.17 $\pm$ 0.02	72 $\pm$ 2.1	24 $\pm$ 1.2	23 $\pm$ 2.0	21 $\pm$ 1.3	281 $\pm$ 15
2020	Control	2.60 $\pm$ 0.05	0.111 $\pm$ 0.003	0.41 $\pm$ 0.04	4.20 $\pm$ 0.11	0.49 $\pm$ 0.01	0.09 $\pm$ 0.01	61 $\pm$ 2.6	22 $\pm$ 0.8	25 $\pm$ 1.1	19 $\pm$ 1.3	234 $\pm$ 14
	OXY	2.63 $\pm$ 0.02	0.112 $\pm$ 0.002	0.40 $\pm$ 0.04	4.45 $\pm$ 0.15	0.45 $\pm$ 0.01	0.08 $\pm$ 0.01	62 $\pm$ 2.2	25 $\pm$ 1.6	27 $\pm$ 1.7	20 $\pm$ 0.8	268 $\pm$ 12
2021	Control	2.87 $\pm$ 0.04	0.145 $\pm$ 0.003	0.41 $\pm$ 0.03	4.91 $\pm$ 0.09	0.57 $\pm$ 0.01	0.09 $\pm$ 0.01	80 $\pm$ 4.2	21 $\pm$ 2.1	20 $\pm$ 0.8	26 $\pm$ 1.1	289 $\pm$ 10
	OXY	2.93 $\pm$ 0.03	0.143 $\pm$ 0.004	0.41 $\pm$ 0.04	5.01 $\pm$ 0.08	0.56 $\pm$ 0.01	0.09 $\pm$ 0.01	86 $\pm$ 4.4	20 $\pm$ 1.6	21 $\pm$ 1.5	26 $\pm$ 0.9	300 $\pm$ 9
ANOVA												
Treatment		ns	ns	ns	ns	**	ns	ns	ns	ns	ns	
Year		***	***	ns	***	***	***	***	***	***	**	
Treatment $\times$ Year		ns	ns	ns	ns	ns	ns	ns	ns	ns	ns	

ns, \*\*, and \*\*\* indicate non-significant differences,  $p < 0.01$ , and  $p < 0.001$ , respectively.  $p$ -values correspond to the effects of treatment, year, and their interaction obtained from factorial repeated-measures ANOVA in a mixed-model framework.

**Table 8.** Yield parameters (yield, fruit load, and mean fruit weight) and crop water use efficiency (YWUE) for each treatment (Control and OXY) during the experimental period (2018–2021). Values are means  $\pm$  standard error (SE,  $n = 12$  trees per treatment and year).

Year	Treatment	Yield (kg Tree $^{-1}$ )	Fruit Load (nº Fruit Tree $^{-1}$ )	Fruit Weight (g)	YWUE (kg m $^{-3}$ )
2018	Control	77.9 $\pm$ 8.4	416 $\pm$ 56	197.9 $\pm$ 8.0	11.0 $\pm$ 1.20
	OXY	79.3 $\pm$ 6.2	421 $\pm$ 45	199.0 $\pm$ 10.8	12.1 $\pm$ 0.95
2019	Control	53.0 $\pm$ 9.3	270 $\pm$ 51	211.8 $\pm$ 9.8	8.4 $\pm$ 1.48
	OXY	64.6 $\pm$ 10.1	336 $\pm$ 55	198.2 $\pm$ 8.8	10.2 $\pm$ 1.59
2020	Control	64.6 $\pm$ 7.2	404 $\pm$ 52	168.8 $\pm$ 7.9	9.6 $\pm$ 1.07
	OXY	79.2 $\pm$ 7.1	548 $\pm$ 61	152.0 $\pm$ 6.9	11.8 $\pm$ 1.06
2021	Control	93.6 $\pm$ 7.4	635 $\pm$ 56	150.1 $\pm$ 5.2	16.4 $\pm$ 1.30
	OXY	103.1 $\pm$ 8.8	725 $\pm$ 78	146.8 $\pm$ 5.2	18.1 $\pm$ 1.55
2018–2021	Accumulated		Accumulated	Mean	Mean
	Control	289.1 $\pm$ 27.3	1725 $\pm$ 174	170.6 $\pm$ 4.3	11.2 $\pm$ 1.06
	OXY	326.2 $\pm$ 26.1	2030 $\pm$ 178	162.7 $\pm$ 3.3	12.9 $\pm$ 1.03
ANOVA					
Treatment		ns	*	ns	*
Year		***	***	***	***
Treatment $\times$ Year		ns	ns	ns	ns

ns, \*, and \*\*\* indicate non-significant differences,  $p < 0.05$ , and  $p < 0.001$ , respectively.  $p$ -values correspond to the effects of treatment, year, and their interaction obtained from factorial repeated-measures ANOVA in a mixed-model framework. Accumulated and mean values are presented for descriptive purposes and were not included in the ANOVA.

### 3.3.6. Fruit Quality

Oxyfertigation may influence specific aspects of fruit quality in ‘Ortanique’ mandarin trees’ development and composition (Table 9). Fruit physical attributes (diameter, height, and external color index) showed strong interannual variation ( $p < 0.001$ ) but were not significantly affected by treatment or treatment  $\times$  year interaction. Peel thickness exhibited a significant year effect ( $p < 0.001$ ) and a modest treatment  $\times$  year interaction ( $p < 0.05$ ), with OXY-treated fruit showing slightly thicker peels in 2018 and 2021, whereas differences were reduced in 2019 and absent in 2020.

Juice percentage displayed the strongest treatment  $\times$  year response ( $p < 0.001$ ). In 2019 and 2020, fruit from OXY trees had significantly lower juice content than controls while no treatment effect occurred in 2018 or 2021. These shifts were mirrored by pulp proportion, which varied across seasons ( $p < 0.001$ ) without a significant interaction, and by peel proportion, where a clear treatment  $\times$  year interaction was detected ( $p < 0.001$ ) due to alternating shifts in peel allocation between treatments across years.

Total soluble solids (TSS) were mainly driven by year ( $p < 0.001$ ) and showed a weak treatment  $\times$  year interaction ( $p < 0.05$ ), with OXY-treated fruit displaying slightly higher TSS in 2020 but lower values in 2019. Titratable acidity increased significantly in OXY fruits ( $p < 0.01$ ) and was strongly influenced by year ( $p < 0.001$ ), although no treatment  $\times$  year interaction was detected. The maturity index decreased significantly under oxyfertigation ( $p < 0.05$ ) and exhibited a pronounced year effect ( $p < 0.001$ ), but no treatment  $\times$  year interaction was observed.

Taken together, fruit quality was dominated by seasonal drivers, with only episodic treatment effects that did not persist across years. Oxyfertigation influenced specific compositional traits such as juice percentage, peel allocation, acidity, and maturity index in certain seasons, but did not consistently modify whole-fruit physical or organoleptic quality across the experimental period.

**Table 9.** Fruit quality parameters (diameter, height, external color index, peel thickness, juice, pulp and peel contents, total soluble solids, titratable acidity, and maturity index) of ‘Ortanique’ mandarin fruits for each irrigation treatment (Control and OXY) during the experimental period (2018–2021). Values are means  $\pm$  standard error (SE,  $n = 12$  trees per treatment and year).

Year	Treatment	Diameter (mm)	Height (mm)	External Color Index	Peel Thickness (mm)	Juice (%)	Pulp (%)	Peel (%)	Total Soluble Solids ( $^{\circ}$ Brix)	Titratable Acidity (g L $^{-1}$ )	Maturity Index
2018	Control	80.5 $\pm$ 0.8	64.4 $\pm$ 0.7	19.8 $\pm$ 0.2	3.05 $\pm$ 0.09 bc	54.8 $\pm$ 0.5 a	3.4 $\pm$ 0.12	41.6 $\pm$ 0.6 c	12.4 $\pm$ 0.2 bc	11.4 $\pm$ 0.3	10.0 $\pm$ 0.20
	OXY	81.6 $\pm$ 1.4	64.7 $\pm$ 0.9	20.5 $\pm$ 0.2	3.24 $\pm$ 0.09 ab	52.7 $\pm$ 0.8 a	3.3 $\pm$ 0.14	43.5 $\pm$ 0.8 c	12.2 $\pm$ 0.2 c	12.6 $\pm$ 0.2	9.7 $\pm$ 0.18
2019	Control	82.0 $\pm$ 0.8	65.0 $\pm$ 0.7	20.1 $\pm$ 0.4	3.34 $\pm$ 0.11 a	48.5 $\pm$ 0.9 b	2.8 $\pm$ 0.16	47.7 $\pm$ 1.0 b	11.1 $\pm$ 0.1 d	12.7 $\pm$ 0.3	8.1 $\pm$ 0.19
	OXY	80.8 $\pm$ 0.9	64.2 $\pm$ 0.9	19.6 $\pm$ 0.2	3.15 $\pm$ 0.08 abc	43.3 $\pm$ 1.4 d	2.7 $\pm$ 0.06	53.0 $\pm$ 1.4 a	10.9 $\pm$ 0.2 d	14.7 $\pm$ 0.2	7.4 $\pm$ 0.15
2020	Control	75.7 $\pm$ 2.1	58.9 $\pm$ 1.8	18.8 $\pm$ 0.7	2.74 $\pm$ 0.08 de	42.9 $\pm$ 0.8 d	4.6 $\pm$ 0.81	51.4 $\pm$ 0.1 a	12.6 $\pm$ 0.20 bc	16.1 $\pm$ 0.3	7.3 $\pm$ 0.13
	OXY	74.5 $\pm$ 1.7	57.8 $\pm$ 1.5	19.3 $\pm$ 0.5	2.51 $\pm$ 0.11 e	45.2 $\pm$ 0.8 cd	4.7 $\pm$ 0.90	49.0 $\pm$ 0.1 b	13.4 $\pm$ 0.3 a	18.7 $\pm$ 0.6	7.2 $\pm$ 0.20
2021	Control	76.2 $\pm$ 1.2	57.2 $\pm$ 0.8	16.5 $\pm$ 0.3	2.65 $\pm$ 0.07 e	48.1 $\pm$ 0.7 b	2.4 $\pm$ 0.07	48.4 $\pm$ 0.6 b	12.6 $\pm$ 0.1 bc	15.1 $\pm$ 0.2	7.7 $\pm$ 0.09
	OXY	75.2 $\pm$ 0.9	56.3 $\pm$ 0.5	17.0 $\pm$ 0.3	2.98 $\pm$ 0.08 cd	47.2 $\pm$ 0.5 bc	2.9 $\pm$ 0.20	48.8 $\pm$ 0.6 b	12.9 $\pm$ 0.2 ab	16.9 $\pm$ 0.5	7.7 $\pm$ 0.16
ANOVA											
Treatment		ns	ns	ns	ns	*	ns	*	ns	**	*
Year		***	***	***	***	***	***	***	***	***	***
Treatment $\times$ Year		ns	ns	ns	*	***	ns	***	*	ns	ns

ns, \*, \*\* and \*\*\* indicate non-significant differences,  $p < 0.05$ ,  $p < 0.01$  and  $p < 0.001$ , respectively. Different lowercase letters within a column indicate significant differences among year  $\times$  treatment combinations according to Duncan’s test ( $p < 0.05$ ).  $p$ -values correspond to the effects of treatment, year, and their interaction obtained from factorial repeated-measures ANOVA in a mixed-model framework.

## 4. Discussion

This study provided one of the first long-term field assessments of oxyfertigation in mature citrus trees under Mediterranean semi-arid conditions. Our working hypothesis proposed that increasing the concentration of dissolved oxygen in irrigation water through the application of  $H_2O_2$  would enhance soil aeration, stimulate root activity, and improve physiological performance and YWUE in mature citrus trees. In the present study, the continuous application of  $H_2O_2$  through irrigation water significantly increased the DO concentration and ODR in the soil (Figure 2), confirming the first part of the hypothesis, showing that oxyfertigation effectively improves rhizosphere aeration under field conditions and establishes the basis for a physiological and agronomic study.

### 4.1. Soil Oxygenation and Microbial Response

Oxyfertigation with  $H_2O_2$  markedly increased dissolved oxygen (DO) in irrigation water and soil oxygen diffusion rate (ODR), confirming its effectiveness in improving rhizosphere aeration under drip irrigation, the first part of the hypothesis (Figure 2). However, we did not measure continuous soil  $O_2$  profiles or redox potential; rhizosphere oxygen status was inferred from ODR and DO in irrigation water. The significant treatment  $\times$  DOY interaction for DO in both years, and for ODR in 2021, indicates that these effects were episodic and more evident under conditions favoring  $O_2$  depletion, such as high soil moisture and temperature. This agrees with the dynamic nature of soil aeration, strongly influenced by irrigation frequency, texture, and evaporative demand [55]. Our results align with previous findings in hydroponic and soil systems, where  $H_2O_2$  decomposition rapidly increased  $O_2$  availability [29,30]. Similar responses were reported in field soils with high organic matter [25], although the magnitude was lower than in controlled environments, likely due to slower  $O_2$  diffusion and higher microbial consumption typical of orchard soils. This suggests that soil texture and organic matter modulate oxyfertigation efficiency under real conditions. Importantly, oxyfertigation did not permanently alter seasonal aeration patterns but alleviated short-term hypoxia during periods of restricted gas exchange. Therefore, it should be considered a complementary practice to mitigate transient aeration constraints rather than a structural modifier of root physiology in mature citrus orchards under semi-arid conditions.

Soil  $CO_2$  and  $H_2O$  vapor fluxes exhibited strong seasonal dynamics (Figure 3), peaking in late spring and declining toward summer, driven mainly by soil temperature and moisture [56–58]. Repeated-measures ANOVA confirmed that day of year was the dominant factor ( $p < 0.001$ ) while treatment and its interaction with time were not significant. Thus, oxyfertigation did not alter the overall trajectory of soil gas fluxes, which remained controlled by environmental conditions and irrigation regime. Occasional increases in  $CO_2$  and  $H_2O$  fluxes under OXY in 2020 suggest the transient stimulation of microbial or root respiration when improved aeration coincided with favorable moisture and temperature, but these effects were not sustained. This agrees with evidence that  $O_2$ -enriched irrigation enhances soil respiration only under suboptimal aeration and that responses are episodic, modulated by soil physical properties and water content [59–61]. In our calcareous orchard, chronic hypoxia was unlikely; oxyfertigation acted as a situational enhancer rather than a structural driver of seasonal  $CO_2$  efflux.

Beyond physical aeration, oxyfertigation showed a limited impact on major microbial groups: aerobic mesophiles and actinomycetes remained unaffected (Table 4), indicating that the transient release of  $O_2$  and reactive species during  $H_2O_2$  decomposition did not induce stable population shifts. In contrast, *Tylenchulus* spp. densities were consistently lower under OXY across seasons, without treatment  $\times$  year interaction, suggesting a robust effect under varying conditions. This nematode is a key citrus pest linked to reduced root

function and vigor [62–64]. The nematicidal properties of  $\text{H}_2\text{O}_2$ , previously documented for *Meloidogyne javanica* on tomato [65], support the hypothesis that oxidative stress and hydroxyl radicals impair nematode survival. Saprophytic nematodes were not affected, indicating that oxyfertigation did not disrupt free-living nematode communities, which play a key role in nutrient cycling and soil food-web dynamics [66,67]. This selective suppression of phytoparasitic nematodes, combined with neutrality toward beneficial groups, is ecologically advantageous and positions oxyfertigation as a potential complementary tool in integrated pest management. From an agronomic perspective, this dual effect, improved aeration and reduced parasitic nematodes, adds value beyond physiological benefits. However, spatial heterogeneity and the short monitoring window warrant multi-year, multi-site validation to confirm reliability and economic relevance. Finally, the year effect observed for molds and yeasts reflects strong climatic control over fungal activity, consistent with previous reports linking heterotrophic dynamics to moisture pulses and temperature variability [56,68]. In addition to this climatic influence, a progressive acclimation of microbial communities may also have attenuated the stimulatory effect of oxyfertigation in 2021, reducing treatment contrasts relative to 2020.

#### 4.2. Nutrient Dynamics and Soil-Plant Interactions

Oxyfertigation with  $\text{H}_2\text{O}_2$  did not significantly alter salinity or basic fertility in this calcareous citrus soil. Electrical conductivity, chloride, sulfate, and exchangeable  $\text{Na}^+$  remained low and statistically similar between treatments (Table 2), indicating that  $\text{H}_2\text{O}_2$  addition did not induce secondary salinization or disrupt ionic balance. This stability agrees with reports from Mediterranean citrus orchards on calcareous Fluvisols, where high carbonate content and moderate CEC buffer short-term changes in EC and exchangeable cations under drip irrigation [69]. Year effects on pH, active  $\text{CaCO}_3$ , organic matter, and organic C, independent of treatment, reflect the dominant influence of climate and management over any direct impact of oxyfertigation. Similar interannual shifts in pH and organic fractions have been documented in irrigated Mediterranean orchards, driven by rainfall variability, residue inputs, and tillage against a chemically buffered calcareous matrix [69].

Macronutrient and micronutrient contents in the 0–30 cm layer showed no treatment effect and only limited year effects for assimilable P and B (Table 3). The decline in Olsen P in 2021 was consistent with crop uptake and P fixation in carbonate-rich soils, where Ca–P precipitation and sorption drive fluctuations in available P according to fertilization and moisture regime rather than small changes in root-zone aeration [70]. Conversely, the marked increase in extractable B reflected its high sensitivity to irrigation quality and episodic leaching by intense rainfall, leading to temporal accumulation or dilution without major changes in other nutrients [70]. These findings indicate that soil nutrient availability and salinity were primarily controlled by soil type, climate, and irrigation water quality while oxyfertigation with  $\text{H}_2\text{O}_2$  behaved as a chemically neutral practice at the soil level.

Taken together, soil and leaf data indicate that oxyfertigation was chemically and nutritionally neutral under the conditions of this study. Physiological and agronomic responses were therefore mediated not by changes in bulk nutrient supply but by improved rhizosphere oxygenation.

#### 4.3. Plant Physiological Responses

Seasonal patterns of midday stem water potential ( $\Psi_{\text{stem}}$ ) were driven mainly by environmental factors rather than oxyfertigation. The day of the year had a highly significant effect in all seasons while treatment and its interaction with time were generally non-significant, except in 2018, when a transient interaction suggested the short-term miti-

gation of midday stress under OXY during periods of high evaporative demand and soil moisture (Figure 4A,D). This behavior aligns with the well-documented sensitivity of citrus water status to atmospheric demand and soil water availability in drip-irrigated orchards, where  $\Psi_{\text{stem}}$  closely tracks vapor pressure deficit and irrigation regime, and only diverges between treatments under strong or prolonged water deficits [71]. In this study, irrigation scheduling maintained favorable soil moisture, so root hypoxia was likely intermittent, and additional  $O_2$  from  $H_2O_2$  did not produce a persistent difference in  $\Psi_{\text{stem}}$ .

Similarly, seasonal gas exchange patterns were dominated by environmental drivers, and oxyfertigation did not consistently modify whole-season physiological performance (Figure 5). Occasional treatment differences suggest that improved aeration may transiently stimulate leaf gas exchange under specific conditions, but these responses were episodic and did not accumulate into sustained physiological gains. Increases in  $g_s$  and  $E_{\text{leaf}}$  indicate improved stomatal regulation and water transport while higher  $A_{CO_2}$  reflects greater photosynthetic efficiency. Comparable short-term improvements have been reported in grapevine [25] and potato [33], where moderate  $H_2O_2$  doses have enhanced photosynthesis and root aeration.

Seasonal variation in leaf water use efficiency was pronounced across all years, reflecting strong environmental control rather than treatment effects (Figure 6). Statistical analysis confirmed significant day effects while treatment and its interaction with time were non-significant. Occasional differences at specific dates suggest that improved aeration may briefly influence stomatal behavior and the carbon–water balance, but these responses were short-lived and did not accumulate into sustained improvements. This pattern is consistent with findings in Mediterranean orchards, where leaf water use efficiency is primarily governed by vapor-pressure deficit and soil moisture [71,72]. Similar context-dependent responses have been reported in woody crops under oxygen-enriched irrigation, where physiological benefits were transient and did not translate into long-term gains [37]. The lack of sustained gains in leaf-scale WUE under OXY likely reflects a disproportionate increase in stomatal conductance and transpiration relative to  $CO_2$  assimilation, a response consistent with the conservative water-use strategy of citrus, where stomata are highly sensitive to atmospheric demand. Under the conditions of this study, oxyfertigation provided only short-term improvements in leaf water use efficiency without generating sustained benefits throughout the season.

Vegetative growth responses were more consistent than physiological ones. The significant treatment effect detected for fresh pruning biomass indicates that oxyfertigation enhanced canopy vigor (Table 5). Higher pruning weights under OXY across seasons suggest greater shoot and leaf production, likely supported by the transient improvements in water status and gas exchange observed earlier. Comparable long-term biomass gains have been reported in avocado and cotton following  $H_2O_2$  application [32,35], reinforcing the idea that improved rhizosphere oxygenation can gradually favor carbon allocation in perennial species. The absence of a treatment  $\times$  year interaction for pruning biomass shows that this stimulatory effect was relatively stable across seasons despite marked interannual variability in absolute values. From an agronomic perspective, increased vegetative growth under oxyfertigation may benefit canopy renewal and future fruiting potential, although it could also require more intensive pruning management. In contrast, trunk growth was strongly influenced by year, reflecting the dominant role of tree age, climate, and seasonal growth dynamics. The progressive decline from 2018 to 2021 is consistent with the physiological behavior of mature citrus trees, where radial growth decreases as trees approach full canopy development [73].

No significant differences in root dry weight were detected between treatments (Table 6), which is consistent with the high spatial heterogeneity typical of mature cit-

rus root systems. Local variability in soil structure, water availability, and emitter position generates strong vertical and horizontal differences in root density, with coefficients of variation often exceeding 40–50% even within a single management unit [74]. This heterogeneity, combined with the limited number of soil cores that can be sampled destructively in commercial orchards, makes detecting treatment effects difficult unless differences are very large.

In this study, thick root biomass and total root dry weight tended to be higher under oxyfertigation, especially in the 15–30 cm layer, but variability prevented statistical significance. This trend is physiologically plausible and aligns with evidence from O<sub>2</sub>-enriched irrigation, where improved rhizosphere aeration enhanced root growth and aboveground biomass [5,25,35]. Fine roots in citrus are highly sensitive to hypoxia, supporting the hypothesis that alleviating transient O<sub>2</sub> limitations near emitters may favor secondary root development and deeper soil exploration, even if responses are not uniform across trees [5]. Under the conditions of this study, oxyfertigation did not produce a statistically robust effect at the orchard scale, and the observed variability highlights the need for integrative approaches, such as minirhizotrons, ground-penetrating methods, or repeated coring, to accurately quantify root responses in future experiments.

#### 4.4. Agronomic Responses: Yield and Fruit Quality

Yield data over four seasons show that oxyfertigation did not significantly increase fruit yield in the short term although a gradual positive trend was evident (Table 8). As shown in Figure S1 and Table S13, most orchard-scale effect sizes for yield fell within the small-to-moderate range, with the fruit number approaching moderate in specific years. Consistently higher yields under OXY suggest a modest productive response, with effect sizes in the small-to-moderate range, similar to cumulative gains reported in grapevine and avocado under O<sub>2</sub>-enriched irrigation [25,35]. The smaller magnitude observed in citrus likely reflects its deeper rooting pattern and greater soil O<sub>2</sub>-buffering capacity, which delay the translation of physiological improvements into agronomic outcomes. Fruit load responded significantly to oxyfertigation, with OXY trees producing more fruits per tree across seasons. This indicates that improved root-zone aeration favored reproductive differentiation and fruit set rather than individual fruit growth, as supported by the absence of treatment effects on mean fruit weight and the slight compensatory reduction in fruit size under OXY.

The significant increase in YWUE under OXY indicates improved irrigation efficiency. Although yield gains were not statistically significant, the combination of higher fruit load and similar water inputs resulted in more kilograms of fruit per cubic meter of water. This suggests that oxyfertigation can enhance water use efficiency at the orchard scale, even when absolute yield responses remain modest. Cumulative increases of approximately 13% in fruit yield and 18% in fruit number under OXY are biologically relevant for perennial crops such as citrus. Even moderate improvements can translate into meaningful benefits over multiple seasons, particularly in semi-arid regions where water scarcity and production costs are critical.

Year effects dominated all yield-related parameters, reflecting the strong influence of climate, tree physiology, and seasonal water availability. The marked increase in yield and YWUE in 2021 compared with previous years illustrates favorable environmental conditions and cumulative physiological effects linked to tree age and canopy development. However, the absence of treatment  $\times$  year interactions for yield, fruit load, fruit weight, and YWUE indicates that oxyfertigation effects were consistent across seasons and not dependent on specific annual conditions. This stability supports the interpretation that increases in fruit load and YWUE are structurally linked to oxyfertigation.

From an agronomic and economic perspective, these trends suggest that oxyfertigation could improve orchard sustainability by reducing risks associated with root hypoxia and supporting resource-use efficiency. For commercial orchards, a 10–15% increase in cumulative yield combined with lower water consumption per kilogram of fruit could enhance profitability and water savings, warranting future cost-benefit assessments to evaluate the feasibility of integrating  $H_2O_2$  application into precision irrigation programs. Future research should include cost-benefit assessments to determine the economic feasibility of integrating  $H_2O_2$  application into precision irrigation programs.

While oxyfertigation showed consistent improvements in YWUE and fruit load, its influence on fruit quality was far less evident. Fruit quality was mainly driven by interannual variability, while oxyfertigation effects were modest and inconsistent (Table 9). This agrees with evidence that climate, phenology, and irrigation patterns often dominate over management practices in determining citrus composition and maturity [75,76]. By year, OXY fruit showed lower juice percentage in 2019 and 2020, slightly higher TSS in 2020 but lower in 2019, higher titratable acidity in multiple years, and alternating peel allocation (thicker peel in 2019 and thinner in 2020), in line with significant treatment  $\times$  year effects. These occasional interactions suggest that  $O_2$  enrichment may influence fruit composition under specific conditions, but these effects were not recurrent. Similar variability has been reported in deficit irrigation studies, where transient improvements in TSS or TA have depended on the timing and severity of soil-water conditions [77,78]. Our findings reinforce that fruit composition is primarily controlled by environmental dynamics at orchard scale.

The inconsistent effects of oxyfertigation reflect the aeration conditions typical of drip-irrigated citrus orchards in semi-arid soils, where root hypoxia is intermittent rather than chronic. Under these circumstances,  $O_2$  enrichment may only influence fruit traits when transient aeration limitations coincide with sensitive phenological stages without producing consistent quality changes across seasons. Similar findings have been reported in citrus studies where irrigation strategies improved tree physiology without recurrent quality gains [76]. Therefore, oxyfertigation should be regarded as a complementary practice with context-dependent effects, while in mature orchards with efficient drip irrigation, fruit quality is primarily driven by seasonal climate and irrigation scheduling.

## 5. Conclusions

Over four consecutive seasons, chemical oxyfertigation with  $H_2O_2$  increased dissolved oxygen in irrigation water and enhanced soil oxygen diffusion dynamics under drip-irrigated citrus. These oxygenation effects were associated with transient increases in soil microbial respiration and with short-term improvements in gas exchange performance. However, the whole-tree water status, soil mineral composition, root biomass allocation, and leaf nutrient content showed high seasonal variability and no sustained treatment effects when evaluated using repeated-measures factorial analysis.

Yield parameters presented consistent positive trends in favor of oxyfertigation, although not statistically significant at the whole-tree scale. Importantly, oxyfertigation promoted a more efficient allocation of assimilates towards reproductive output, significantly increasing the fruit number and YWUE, while the absence of a consistent effect on fruit size and total yield reflected the complex source–sink balances and compensation mechanisms characteristic of mature citrus orchards.

Taken together, these results indicate that oxyfertigation is more likely to provide transient or condition-specific benefits rather than systematic improvements in mature citrus orchards under semi-arid drip irrigation. The technique may improve physiological performance or soil aeration during windows of elevated environmental demand or

reduced natural oxygen availability but does not consistently modify plant water status, canopy growth, or fruit quality when analyzed over multiple seasons.

Future research should focus on identifying the environmental and soil conditions under which oxyfertigation delivers the greatest agronomic value, including situations of chronic hypoxia, heavier soils, salinity constraints, reduced irrigation percolation, or regenerative systems with limited tillage. Multi-factor experiments integrating oxygen enrichment, irrigation scheduling and soil structure management will be essential to clarify whether cumulative or synergistic effects can be achieved at the crop-system scale.

**Supplementary Materials:** The following supporting information can be downloaded at: <https://www.mdpi.com/article/10.3390/agriculture16010075/s1> Table S1: Soil mineral content (salinity) for each irrigation treatment (Control and OXY) during the two last seasons (2020 and 2021). Values are means  $\pm$  standard error (SE) and 95% confidence intervals (95% CI). Table S2: Soil mineral content (soil reaction and organic matter) for each irrigation treatment (Control and OXY) during the two last seasons (2020 and 2021). Values are means  $\pm$  standard error (SE) and 95% confidence intervals (95% CI). Table S3: Soil mineral content (primary macronutrients) for each irrigation treatment (Control and OXY) during the two last seasons (2020 and 2021). Values are means  $\pm$  standard error (SE) and 95% confidence intervals (95% CI). Table S4: Soil mineral content (secondary macronutrients, micronutrients and cation exchange capacity) for each irrigation treatment (Control and OXY) during the two last seasons (2020 and 2021). Values are means  $\pm$  standard error (SE) and 95% confidence intervals (95% CI). Table S5: Soil microbiology and nematode phytopathology for each irrigation treatment (Control and OXY) during the two last seasons (2020 and 2021). Values are means  $\pm$  standard error (SE) and 95% confidence intervals (95% CI). Table S6: Absolute growth rate of the trunk cross-sectional area (AGR<sub>Trunk</sub>,  $\text{cm}^2 \text{ year}^{-1}$ ) and fresh pruning weight ( $\text{kg tree}^{-1}$ ) for each irrigation treatment (Control and OXY) during the experimental period (2018–2021). Values are means  $\pm$  standard error (SE) and 95% confidence intervals (95% CI). Table S7: Root dry weight ( $\times 10^2 \text{ g cm}^{-3}$ ) of fine and thick roots at two soil depths for each treatment (Control and OXY) at the end of the experimental period (November 2021). Values are means  $\pm$  standard error (SE) and 95% confidence intervals (95% CI). Table S8: Leaf mineral content of ‘Ortanique’ mandarin trees for each irrigation treatment (Control and OXY) during the experimental period (2018–2021). Primary macronutrients (N, P and K) and secondary macronutrients (Ca, Mg and Na). Values are means  $\pm$  standard error (SE) and 95% confidence intervals (95% CI). Table S9: Leaf mineral content (microelements) of ‘Ortanique’ mandarin trees for each irrigation treatment (Control and OXY) during the experimental period (2018–2021). Values are means  $\pm$  standard error (SE) and 95% confidence intervals (95% CI). Table S10: Yield parameters (yield, fruit load, and mean fruit weight) and agronomic water use efficiency (YWUE) for each treatment (Control and OXY) during the experimental period (2018–2021). Values are means  $\pm$  standard error (SE) and 95% confidence intervals (95% CI). Table S11: Fruit quality parameters (diameter, height, external color index, and peel thickness) of ‘Ortanique’ mandarin fruits for each irrigation treatment (Control and OXY) during the experimental period (2018–2021). Values are means  $\pm$  standard error (SE) and 95% confidence intervals (95% CI). Table S12: Fruit quality parameters (juice, pulp and peel contents, total soluble solids, titratable acidity and maturity index) of ‘Ortanique’ mandarin fruits for each irrigation treatment (Control and OXY) during the experimental period (2018–2021). Values are means  $\pm$  standard error (SE) and 95% confidence intervals (95% CI). Table S13: Effect sizes (Cohen’s d and Hedges’ g) by year and accumulated (2018–2021) for yield, fruit number, mean fruit weight, and crop water use efficiency (YWUE). Figure S1: Hedges’ g effect sizes by year (2018–2021) and accumulated (2018–2021) for yield, fruit number, mean fruit weight, and YWUE. Horizontal dashed lines mark interpretation thresholds (0.2 = small, 0.5 = moderate, 0.8 = large).

**Author Contributions:** Conceptualization, J.M.R. and J.G.P.-P.; methodology, J.M.R., J.G.P.-P. and J.M.N.; formal analysis, J.M.R., J.G.P.-P. and F.M.H.-B.; investigation, J.M.R., J.G.P.-P., F.M.H.-B. and E.I.M.; data curation, J.M.R.; writing—original draft preparation, J.M.R.; J.G.P.-P., F.M.H.-B. and J.M.N.; writing—review and editing, J.M.R., J.G.P.-P., J.M.N., E.I.M. and P.B.; supervision, J.M.R. and

J.G.P.-P.; funding acquisition, J.M.R. All authors have read and agreed to the published version of the manuscript.

**Funding:** This research was funded by the FEDER 1420-13 and FEDER 1420-24 project (operating program of the Region of Murcia 2014–2020), co-financed at 80% by the European Regional Development Fund, and by the Subprogram for Hiring and Incorporation of Doctors INIA-CCAA (DR13-0170), as well as by the State Subprogram for Ramón y Cajal Incorporation (RYC-2015-17726), within the framework of the State Plan for Scientific and Technical Research and Innovation of the Ministry of Economy and Competitiveness.

**Institutional Review Board Statement:** Not applicable.

**Data Availability Statement:** Data are contained within the article and its Supplementary Materials.

**Acknowledgments:** The authors want to thank J.A. Palazón, E.M. Arques, and L. Campana for their help in both field and laboratory tasks and the Campo de Cartagena Irrigation Community for the availability of the experimental orchard.

**Conflicts of Interest:** The authors declare no conflicts of interest. The funders had no role in the design of the study; in the collection, analyses, or interpretation of data; in the writing of the manuscript; or in the decision to publish the results.

## Abbreviations

The following abbreviations have been used in this manuscript:

$H_2O_2$	Hydrogen peroxide
YWUE	Crop water use efficiency
IMIDA	Instituto Murciano de Investigación y Desarrollo Agrario y Medioambiental
EC	Electrical conductivity
$ET_0$	Reference evapotranspiration
$ET_c$	Crop evapotranspiration
$K_c$	Crop coefficient
VPD	Vapor Pressure Deficit
DO	Dissolved oxygen
ODR	Soil oxygen diffusion rate
CEC	Cation exchange capacity
$\Psi_{stem}$	Midday stem water potential
$A_{CO2}$	Net photosynthesis rate
$g_s$	Stomatal conductance
$E_{leaf}$	Leaf transpiration rate
$A_{CO2}/E_{leaf}$	Instantaneous leaf water use efficiency
$A_{CO2}/g_s$	Intrinsic leaf water use efficiency
TCSA	Trunk cross-sectional area
$AGR_{trunk}$	Absolute growth rate of the TCSA

## References

1. MAPA. Anuario de Estadística Agraria 2023. Ministerio de Agricultura, Pesca y Alimentación. Available online: <https://www.mapa.gob.es/es/estadistica/temas/publicaciones/anuario-de-estadistica> (accessed on 1 October 2025).
2. CARM. Anuario de Estadística Agraria de Murcia 2023–2024; Consejería de Agua, Agricultura, Ganadería y Pesca, Comunidad Autónoma de la Región de Murcia: Murcia, Spain, 2024.
3. Fernández, J.E.; Alcón, F.; Diaz-Espejo, A.; Hernández-Santana, V.; Cuevas, M.V. Water use indicators and economic analysis for on-farm irrigation decision: A case study of a super high density olive tree orchard. *Agric. Water Manag.* **2020**, *233*, 106074. [[CrossRef](#)]
4. Du, Y.-D.; Niu, W.-Q.; Gu, X.-B.; Zhang, Q.; Cui, B.-J.; Zhao, Y. Crop yield and water use efficiency under aerated irrigation: A meta-analysis. *Agric. Water Manag.* **2018**, *210*, 158–164. [[CrossRef](#)]

5. Li, H.; Junejo, A.R.; Midmore, D.J.; Soomro, S.A. Significance of aerated drip irrigation: A comprehensive review. *Agric. Water Manag.* **2025**, *321*, 109886. [\[CrossRef\]](#)
6. Glinski, J.; Stępniewski, W. *Soil Aeration and Its Role for Plants*, 1st ed.; CRC Press: Boca Raton, FL, USA, 2018; p. 237. [\[CrossRef\]](#)
7. Barret-Lennard, E.G. The interaction between water logging and salinity in higher plants: Causes, consequences and implications. *Plant Soil* **2003**, *253*, 35–54. [\[CrossRef\]](#)
8. Meek, B.D.; Ehlig, C.F.; Stolzy, L.H.; Graham, L.E. Forrow and trickle irrigation: Effects on soil oxygen and ethylene and tomato yield. *Soil Sci. Soc. Am. J.* **1983**, *47*, 631–635. [\[CrossRef\]](#)
9. Bartholomeus, R.P.; Witte, J.P.M.; van Bodegom, P.M.; van Dam, J.C.; Aerts, R. Critical soil conditions for oxygen stress to plant roots: Substituting the Feddes-function by a process-based model. *J. Hydrol.* **2008**, *360*, 147–165. [\[CrossRef\]](#)
10. Navarro, J.M.; Pérez Pérez, J.G. Oxifertirrigación química en el cultivo de plantas de pimiento en condiciones salinas. *Agrícola Vergel* **2019**, *416*, 11–17.
11. Kumar, V.; Butter, T.S.; Samanta, A.; Singh, G.; Kumar, M.; Dhotra, B.; Yadab, N.K.; Choudhary, R.S. Soil compaction and their management in farming systems: A review. *Int. J. Chem. Stud.* **2018**, *6*, 2302–2313.
12. Morales-Olmedo, M.; Ortiz, M.; Selles, G. Effects of transient soil waterlogging and its importance for rootstock selection. *Chil. J. Agric. Res.* **2015**, *75*, 45–56. [\[CrossRef\]](#)
13. Hillel, D. *Environmental Soil Physics: Fundamentals, Applications, and Environmental Considerations*; Academic Press: San Diego, CA, USA, 1998; pp. 1–771.
14. Neira, J.; Ortiz, M.; Morales, L.; Acevedo, E. Oxygen diffusion in soils: Understanding the factors and processes needed for modeling. *Chil. J. Agric. Res.* **2015**, *75*, 35–44. [\[CrossRef\]](#)
15. Letey, J.; Stolzy, L.H. Measurement of oxygen diffusion rates with the platinum microelectrode. I–III. *Hilgardia* **1964**, *35*, 545–576. [\[CrossRef\]](#)
16. Bornstein, J.; Hedstrom, W.E.; Scott, F.R. *Oxygen Diffusion Rate Relationships Under Three Soil Conditions*; Life Sciences and Agriculture Experiment Station: Geneva, NY, USA, 1980; p. 12.
17. Cook, F.J.; Knight, J.H. Oxygen transport to plant roots: Modeling for physical understanding of soil aeration. *Soil Sci. Soc. Am. J.* **2003**, *67*, 20–31. [\[CrossRef\]](#)
18. Cook, F.J.; Knight, J.H.; Kelliher, F.M. Oxygen transport in soil and the vertical distribution of roots. *Aust. J. Soil Res.* **2007**, *45*, 101–110. [\[CrossRef\]](#)
19. Drew, M.C. Oxygen deficiency and root metabolism: Injury and acclimation under hypoxia and anoxia. *Annu. Rev. Plant Physiol. Plant Mol. Biol.* **1997**, *48*, 223–250. [\[CrossRef\]](#)
20. Voesenek, L.A.C.J.; Bailey-Serres, J. Flood adaptive traits and processes: An overview. *New Phytol.* **2015**, *206*, 57–73. [\[CrossRef\]](#)
21. Yamauchi, T.; Colmer, T.D.; Pedersen, O.; Nakazono, M. Regulation of root traits for internal aeration and tolerance to soil waterlogging–flooding stress. *Plant Physiol.* **2018**, *176*, 1118–1130. [\[CrossRef\]](#)
22. Gong, D.H.; Lee, S.H.; Jung, K.Y.; Chun, H.C. Characteristics of Maize Roots under Subsurface Drip Irrigation through Various Oxygen Treatment. *Korean J. Soil Sci. Fertil.* **2023**, *56*, 39–48. [\[CrossRef\]](#)
23. Silberbush, M.; Gornat, B.; Goldberg, D. Effect of irrigation from a point source (trickling) on oxygen flux and on root extension in the soil. *Plant Soil* **1979**, *52*, 507–514. [\[CrossRef\]](#)
24. Bhattarai, S.P.; Su, N.; Midmore, D.J. Oxygation enhances yield and water productivity of vegetables. *Adv. Agron.* **2005**, *88*, 313–377. [\[CrossRef\]](#)
25. Thomas, P.G.; Bhattarai, S.P.; Balsys, R.J.; Walsh, K.B.; Midmore, D.J. Continuous injection of hydrogen peroxide in drip irrigation—Application to field crops. *Agronomy* **2025**, *15*, 385. [\[CrossRef\]](#)
26. Tachikawa, M.; Yamanaka, K. Synergistic disinfection and removal of biofilms by a sequential two-step treatment with ozone followed by hydrogen peroxide. *Water Res.* **2014**, *64*, 94–101. [\[CrossRef\]](#)
27. Japhet, N.; Tarchitzky, J.; Chen, Y. Effectiveness of hydrogen peroxide treatments in preventing biofilm clogging in drip irrigation systems applying treated wastewater. *Biofouling* **2022**, *38*, 575–592. [\[CrossRef\]](#) [\[PubMed\]](#)
28. Palencia, P.; Martínez, F.; Vázquez, M.A. Oxyfertigation and transplanting conditions of strawberries. *Agronomy* **2021**, *11*, 2513. [\[CrossRef\]](#)
29. Urrestarazu, M.; Mazuela, P.C. Effect of slow-release oxygen supply by fertigation on horticultural crops under soilless culture. *Sci. Hortic.* **2005**, *106*, 484–490. [\[CrossRef\]](#)
30. Marfa, O.; Cáceres, R.; Gurí, S. Oxyfertigation: A new technique for soilless culture under Mediterranean conditions. *Acta Hortic.* **2005**, *697*, 65–72. [\[CrossRef\]](#)
31. Acuña, R.; Bonachela, S.; Magán, J. Respuesta de un cultivo de pimiento en sustrato de perlita a la mejora de la oxigenación del medio radicular. *Acta Hortic.* **2006**, *46*, 91–95.
32. Bhattarai, S.P.; Huber, S.; Midmore, D.J. Aerated subsurface irrigation water gives growth and yield benefits to Zucchini, vegetable soybean and cotton in heavy clay soils. *Ann. Appl. Biol.* **2004**, *144*, 285–298. [\[CrossRef\]](#)

33. Abd Elhady, S.A.; El-Gawad, H.G.A.; Ibrahim, M.F.M.; Mukherjee, S.; Elkelish, A.; Azab, E.; Gobouri, A.A.; Farag, R.; Ibrahim, H.A.; El-Azm, N.A. Hydrogen peroxide supplementation in irrigation water alleviates drought stress and boosts growth and productivity of potato plants. *Sustainability* **2021**, *13*, 899. [[CrossRef](#)]

34. Wang, Y.; Shi, W.; Jing, B.; Liu, L. Modulation of soil aeration and antioxidant defenses with hydrogen peroxide improves the growth of winter wheat (*Triticum aestivum* L.) plants. *J. Clean. Prod.* **2024**, *435*, 140565. [[CrossRef](#)]

35. Gil, P.M.; Ferreyra, R.; Barrera, C.; Zúñiga, C.; Gurovich, L. Effect of injecting hydrogen peroxide into heavy clay loam soil on plant water status, net CO<sub>2</sub> assimilation, biomass, and vascular anatomy of avocado trees. *Chil. J. Agric. Res.* **2009**, *69*, 97–106. [[CrossRef](#)]

36. Labanauskas, C.F.; Stolzy, L.H.; Klotz, L.J.; DeWolfe, T.A. Adequate soil-oxygen supplies increase nutrient concentrations in citrus seedlings. *Calif. Agric.* **1964**, *18*, 13–14.

37. Ben-Noah, I.; Nitsan, I.; Cohen, B.; Kaplan, G.; Friedman, S.P. Soil aeration using air injection in a citrus orchard with shallow groundwater. *Agric. Water Manag.* **2021**, *245*, 106664. [[CrossRef](#)]

38. Doorenbos, J.; Pruitt, W.O. *Crop Water Requirements*; FAO Irrigation and Drainage Paper Number 24; FAO: Rome, Italy, 1977; p. 194.

39. Allen, R.G.; Pereira, L.S.; Raes, D.; Smith, M. Crop evapotranspiration. In *Guidelines for Computing Crop Water Requirements*; FAO: Rome, Italy, 1998; p. 56.

40. Boletín Oficial de la Región de Murcia (BORM). Núm 106, 2002, Orden Del 24 de Abril de 2002. In *Por la Que Regulan Las Normas Técnicas de Producción Integrada en el Cultivo de Cítricos; Suplemento Núm 1 Del BORM 9 de Mayo de 2002*; Consejería de Agricultura, Agua y Medio Ambiente: Murcia, Spain, 2002; pp. 188–207.

41. Zhang, Z.; Yang, R.; Zhang, Z.; Geng, Y.; Zhu, J.; Sun, J. Effects of oxygenated irrigation on root morphology, fruit yield, and water–nitrogen use efficiency of tomato (*Solanum lycopersicum* L.). *J. Soil Sci. Plant Nutr.* **2023**, *23*, 5582–5593. [[CrossRef](#)]

42. Yafuso, E.J.; Fisher, P.R. Oxygenation of irrigation water during propagation and container production of bedding plants. *HortScience* **2017**, *52*, 1608–1614. [[CrossRef](#)]

43. Lemon, E.R.; Erickson, A.E. The measurement of oxygen diffusion in the soil with a platinum microelectrode. *Soil Sci. Soc. Am. J.* **1952**, *16*, 160–163. [[CrossRef](#)]

44. Walkley, A.; Black, I. An examination of the Degtjareff method and a proposed modification of the chromic matter and a proposed modification of the chromic acid titration method. *Soil Sci.* **1934**, *34*, 29–38. [[CrossRef](#)]

45. Khaledian, Y.; Brevick, E.C.; Pereira, P.; Cerdá, A.; Fattah, M.A.; Tazikeh, H. Modeling soil cation exchange capacity in multiple countries. *Catena* **2017**, *158*, 194–200. [[CrossRef](#)]

46. Oostenbrink, M. Estimating nematode populations by some selected methods. *Nematology* **1960**, *6*, 85–102.

47. McCutchan, H.; Shackel, K.A. Stem-water potential as a sensitive indicator of water stress in prune trees (*Prunus domestica* L. cv French). *J. Am. Soc. Hortic. Sci.* **1992**, *117*, 607–611. [[CrossRef](#)]

48. Turner, N.C. Measurements of plant water status by pressure chamber technique. *Irrig. Sci.* **1988**, *9*, 289–308. [[CrossRef](#)]

49. Von Caemmerer, S.; Farquhar, G.D. Some relationships between the biochemistry of photosynthesis and the gas exchange of leaves. *Planta* **1981**, *153*, 376–387. [[CrossRef](#)]

50. Sinclair, T.R.; Allen, L.H. Carbon dioxide and water vapour exchange of leaves on field-grown citrus trees. *J. Exp. Bot.* **1982**, *33*, 1166–1175. [[CrossRef](#)]

51. Syvertsen, J.P. Light acclimation in citrus leaves. II. CO<sub>2</sub> assimilation and light, water and nitrogen use efficiency. *J. Am. Soc. Hortic. Sci.* **1984**, *109*, 812–817. [[CrossRef](#)]

52. Ribeiro, R.; Machado, C. Some aspects of citrus ecophysiology in subtropical climates: Re-visiting photosynthesis under natural conditions. *Braz. J. Plant Physiol.* **2007**, *19*, 393–411. [[CrossRef](#)]

53. Pérez-Pérez, J.G.; Robles, J.M.; Botía, P. Effects of deficit irrigation in different fruit growth stages on 'Star Ruby' grapefruit trees in semi-arid conditions. *Agric. Water Manag.* **2014**, *133*, 44–54. [[CrossRef](#)]

54. European Commission. *Regulation (EC) No. 1799/2001 of the Commission of 12 September 2001 Establishing Marketing Standards for citrus*; European Commission: Brussels, Belgium, 2001; Volume 248, pp. 1–45.

55. Grable, A.R. Soil aeration and plant growth. *Adv. Agron.* **1966**, *18*, 57–106. [[CrossRef](#)]

56. Moyano, F.E.; Manzoni, S.; Chenu, C. Responses of soil heterotrophic respiration to moisture availability: An exploration of processes and models. *Soil Biol. Biochem.* **2013**, *59*, 72–85. [[CrossRef](#)]

57. Davidson, E.A.; Janssens, I.A. Temperature sensitivity of soil carbon decomposition and feedbacks to climate change. *Nature* **2006**, *440*, 165–173. [[CrossRef](#)]

58. Vargas, R.; Detto, M.; Baldocchi, D.D.; Allen, M.F. Multiscale analysis of temporal variability of soil CO<sub>2</sub> production as influenced by weather and vegetation. *Glob. Change Biol.* **2010**, *16*, 1589–1605. [[CrossRef](#)]

59. Ben-Noah, I.; Friedman, S.P. Review and evaluation of root respiration and of natural and agricultural processes of soil aeration. *Vadose Zone J.* **2018**, *17*, 180119. [[CrossRef](#)]

60. Ben-Noah, I.; Friedman, S.P. Oxygation of clayey soils by adding hydrogen peroxide to the irrigation solution: Lysimetric experiments. *Rhizosphere* **2016**, *2*, 51–56. [[CrossRef](#)]

61. Yu, Z.; Wang, C.; Zou, H.; Wang, H.; Li, H.; Sun, H.; Yu, D. The effects of aerated irrigation on soil respiration and the yield of the maize root zone. *Sustainability* **2022**, *14*, 4378. [[CrossRef](#)]

62. Verdejo-Lucas, S.; McKenry, M.V. Management of the citrus nematode, *Tylenchulus semipenetrans*. *J. Nematol.* **2004**, *36*, 424–432.

63. Duncan, L.W. Nematode parasites of citrus. In *Plant Parasitic Nematodes in Subtropical and Tropical Agriculture*, 2nd ed.; Luc, M., Sikora, R.A., Bridge, J., Eds.; CABI Publishing: Wallingford, UK, 2005; pp. 437–466. [[CrossRef](#)]

64. Sekora, N.; Crow, W. EENY-529/IN941: Citrus Nematode, *Tylenchulus semipenetrans* (Cobb 1913). *EDIS* **2013**, *2013*, *4*. [[CrossRef](#)]

65. Karajeh, M.R.; Masoud, S.A. Oxamyl and hydrogen peroxide for the control of root-knot nematode *Meloidogyne javanica* on tomato. *J. Plant Prot. Res.* **2008**, *48*, 181–187. [[CrossRef](#)]

66. Neher, D.A. Role of nematodes in soil health and their use as bioindicators. *J. Nematol.* **2001**, *33*, 161–168.

67. Tiwari, S.P. Nematodes and soil health indicators. *Phytopathology* **2017**, *6*, 17–25. [[CrossRef](#)]

68. Collins, S.L.; Sinsabaugh, R.L.; Crenshaw, C.; Green, L.; Porras-Alfaro, A.; Stursova, M.; Zeglin, L.H. Pulse dynamics and microbial processes in aridland ecosystems. *J. Ecol.* **2008**, *96*, 413–420. [[CrossRef](#)]

69. Visconti, F.; Peiró, E.; Baixaúli, C.; de Paz, J.M. Spontaneous plants improve the inter-row soil fertility in a citrus orchard but nitrogen lacks to boost organic carbon. *Environments* **2022**, *9*, 151. [[CrossRef](#)]

70. Acosta, J.A.; Imbernón-Mulero, A.; Martínez-Álvarez, M.; Gallego-Elvira, B.; Maestre-Valero, J.F. Midterm effects of irrigation with desalinated seawater on soil properties and constituents in a Mediterranean citrus orchard. *Agric. Ecosyst. Environ.* **2025**, *381*, 109421. [[CrossRef](#)]

71. Pérez-Pérez, J.G.; Dodd, I.C.; Botía, P. Partial rootzone drying increases water-use efficiency of lemon Fino 49 trees independently of root-to-shoot ABA signalling. *Funct. Plant Biol.* **2012**, *39*, 366–378. [[CrossRef](#)]

72. Medrano, H.; Tomás, M.; Martorell, S.; Flexas, J.; Hernández, E.; Rosselló, J.; Pou, A.; Escalona, J.-M.; Bota, J. From leaf to whole-plant water use efficiency (WUE) in complex canopies: Limitations of leaf WUE as a selection target. *Crop J.* **2015**, *3*, 220–228. [[CrossRef](#)]

73. Ryan, M.G.; Binkley, D.; Fownes, J.H. Age-related decline in forest productivity: Pattern and process. *Adv. Ecol. Res.* **1997**, *27*, 213–262. [[CrossRef](#)]

74. Atta, A.A.; Morgan, K.T.; Kadyampakeni, D.M. Spatial and temporal nutrient dynamics and water management of huanglongbing-affected mature citrus trees on florida sandy soils. *Sustainability* **2022**, *14*, 7134. [[CrossRef](#)]

75. Vélez, J.E.; Álvarez-Herrera, J.G.; Alvarado-Sanabria, O.H. El estrés hídrico en cítricos (*Citrus* spp.): Una revisión. *Orinoquia* **2012**, *16*, 2. [[CrossRef](#)]

76. Berríos, P.; Temnani, A.; Zapata-García, S.; Sánchez-Navarro, V.; Zornoza, R.; Pérez-Pastor, A. Effect of deficit irrigation and mulching on the agronomic and physiological response of mandarin trees as strategies to cope with water scarcity in a semi-arid climate. *Sci. Hortic.* **2024**, *324*, 112572. [[CrossRef](#)]

77. Aguado, A.; Frías, J.; García-Tejero, I.; Romero, F.; Muriel, J.L.; Capote, N. Towards the improvement of fruit-quality parameters in citrus under deficit-irrigation strategies. *ISRN Agron.* **2012**, *2012*, 940896.

78. Gasque, M.; Martí, P.; Granero, B.; González-Altozano, P. Effects of long-term summer deficit irrigation on 'Navelina' citrus trees. *Agric. Water Manag.* **2016**, *169*, 140–147. [[CrossRef](#)]

**Disclaimer/Publisher's Note:** The statements, opinions and data contained in all publications are solely those of the individual author(s) and contributor(s) and not of MDPI and/or the editor(s). MDPI and/or the editor(s) disclaim responsibility for any injury to people or property resulting from any ideas, methods, instructions or products referred to in the content.